Ab initio investigation of the magnetism of tetragonal Mn: Bulk, surface, ultrathin films, and multilayers

J. Hafner* and D. Spišák†
Institut für Materialphysik and Center for Computational Materials Science, Universität Wien, Sensengasse 8, A-1090 Wien, Austria
(Received 14 June 2005; published 24 October 2005)

The magnetic properties of the tetragonally distorted γ and δ phases of Mn stabilized by epitaxial growth on metallic surfaces are still subject of a lively debate, but so far no consistent and generally accepted picture has emerged. We have performed detailed and comprehensive investigations of the geometric and magnetic properties of tetragonal Mn in the bulk, at a (100) surface, in ultrathin Mn/Fe(100) films, and in Mn/Fe multilayers using *ab initio* spin-density functional techniques. The cubic structures of both γ (face-centered cubic) and δ (body-centered cubic) Mn are unstable against tetragonal distortion. Whereas for δ-Mn a structure contracted along the c axis and with $c(2\times2)$ in-plane (100) antiferromagnetism (AFM) is the unique ground state, for γ-Mn a contracted tetragonal ($c/a=0.945$) phase with a layered (100) AFM, and an expanded ($c/a=1.048$) phase with in-plane (100) AFM are energetically almost degenerate. In addition we find that the antiferromagnetic phases of both δ and γ Mn are susceptible to long-period helical modulations. At the (100) surface, the Mn moments are strongly enhanced, and the strong antiferromagnetic coupling between the high surface moments favors in-plane AFM in the surface layer even on top of the tetragonally compressed near-fcc phase stabilizing layered antiferromagnetism in the bulk. A similar result is found for ultrathin Mn/Fe(100) films with up to six monolayers. A strong ferromagnetic Mn/Fe coupling at the interface favors layered antiferromagnetism in the deeper layers, but the in-plane antiferromagnetic structure in the top layer is stable in any case. For the thinnest Mn films we have also examined noncollinear magnetic structures and found evidence for a perpendicular coupling between the Mn surface layer and the deeper layers of film and substrate. The strong ferromagnetic Mn/Fe interface coupling also determines the properties of Fe/Mn multilayers. The ferromagnetic interface coupling is not perturbed by Fe/Mn intermixing and stabilizes a layered antiferromagnetism in the Mn spacer. We discuss our results in the light of the available experimental data and of previous theoretical calculations.

DOI: 10.1103/PhysRevB.72.144420 PACS number(s): 75.10.Lp, 68.55.−a, 68.65.Ac, 75.70.Cn

I. INTRODUCTION

Scientific and technological advances have created new opportunities for designing novel nanostructured materials. Transition-metal clusters, nanowires, ultrathin films, and multilayers can be prepared in a wide variety of compositions, structures, and sizes, providing a large number of new, potentially useful systems. Magnetic properties in particular are found to be extremely sensitive to dimensionality, size, and local environment - nanostructured systems often display magnetic structures and coupling strengths entirely different from their bulk counterparts.[1–3] A very important issue in this field is the coupling of various magnetic materials across an interface, which is closely related to the phenomena of interlayer exchange coupling,[4,5] giant magnetoresistance,[6,7] and to the design of spin-valve systems.[8] Overlayers of antiferromagnetic metals grown on ferromagnetic substrates, such as Cr/Fe(100) (Refs. 9–12) and Mn/Fe(100) (Refs. 13–18) developed to model systems for studying the magnetic properties of such interfaces. Ultrathin layers of Mn grown on Fe(100) substrates in particular are among the most complex and the most extensively studied ferromagnetic/antiferromagnetic interfaces. The interest in this system is triggered by the fact that Fe is the prototypic magnetic metal and in addition because it was expected that in low-dimensional structures Mn atoms could develop an unusually high magnetic moment approaching the gas-phase value of $5\mu_B$. The particular intricacy of the Mn/Fe(100) system arises partly from the unavoidable frustration at a ferromagnetic/antiferromagnetic interface, but mostly from the strange properties of manganese itself. Mn exists in five allotropic forms. The α phase is cubic with 58 atoms in the unit cell (space group $T_d^3-I\bar{4}3m$) at ambient conditions, stable up to 1000 K. At a Néel temperature of $T_N=95$ K, α-Mn undergoes a paramagnetic to antiferromagnetic transition accompanied by a tetragonal distortion of the crystal structure[19] (the space-group symmetry is lowered to $I\bar{4}2m$). The AFM structure of α-Mn is noncollinear, with large magnetic moments (up to $3\mu_B$) on sites I and II, and much smaller moments on the remaining positions, Mn atoms at sites IV may even be nonmagnetic.[19,20] β-Mn is cubic with 20 atoms in the unit cell (space group $P4_132$),[21] stable between 1000 and 1368 K. A face-centered cubic γ phase exists between 1368 and 1406 K, a body-centered δ phase from 1406 K up to the melting point at $T_M=1517$ K. High-pressure studies[22] have revealed a transition to an ϵ phase at about 165 GPa. The structure of ϵ-Mn is probably hexagonal close packed, in agreement with the stable crystal structure of the homologous elements Tc and Re.

The magnetic properties of the high-temperature allotropes can be studied in quenched samples, by extrapolating the data acquired on Mn alloys to zero impurity concentration, or in thin films stabilized by epitaxial growth. Nakamura *et al.*[23] have shown that quenched β-Mn remains mag-

netically disordered down to the lowest temperature (1.4 K) and exhibits strong spin fluctuations. Canals and Lacroix[24] have pointed out that the structure of β-Mn belongs to a family of fully frustrated lattices where the frustration overcomes any magnetic ordering and suggested that it should be considered as a spin liquid. Similar to α-Mn, γ-Mn is antiferromagnetic with a Néel temperature of $T_N=570$ K, the layered antiferromagnetic (type-1 AFM) phase is tetragonally distorted with $c/a=0.946$ (as determined by Endoh and Ishikawa[25] in a study of γ-FeMn and extrapolation to zero Fe content). The determination of the intrinsic magnetic structure of δ-Mn turned out to be more difficult. The growth of Mn films on body-centered cubic substrates (V, Cr, Fe) produces strained tetragonal Mn films whose magnetic properties are still subject of a lively debate—in fact, the properties of these films are one of the major topics of this work.

The strange magnetic properties of Mn are not restricted to the bulk. The surface energies of the 3*d* metals as deduced from the surface tension of the liquid metals by de Boer *et al.*[26] are anomalously low when compared to the nonmagnetic metals of the 4*d* and 5*d* series. In addition, while the surface energies of the heavier transition metals vary parabolically with band filling, with a maximum for a half-filled band, the surface energies of the AFM (Cr, Mn) and FM (Fe, Co, Ni) 3*d* metals are reduced compared to the trends expected from the progressive filling of the band, the strongest anomaly being found for Mn.

It may certainly be considered as a major success of modern local-spin density (LSD) functional theory of itinerant magnetism that the complex correlation between crystal structure and magnetism in the Mn allotropes is now rather well understood. Hobbs *et al.*[27,28] have shown that the strange properties of α-Mn result from the conflicting tendencies to simultaneously maximize the magnetic moment (according to Hund's rule) and the bond strength (as expected for a half-filled *d* band). The α-Mn structure may by considered as an intermetallic compound between strongly magnetic and weakly magnetic Mn atoms. The noncollinear magnetic structure results from the frustrated AFM coupling of weakly magnetic Mn atoms arranged on triangular motifs of the α-Mn structure.[27] In β-Mn, the close-packing constraints are relaxed, but as the Mn atoms are arranged on networks of corner-sharing triangles, the frustration of the AFM coupling is even more pronounced.[28] For the highly symmetric polymorphs, LSD calculations (see Ref. 28 and many further references given therein) show that their equilibrium volume is only slightly larger than the volume for the onset of magnetism. Hexagonal ϵ-Mn is in fact paramagnetic at equilibrium. Fcc γ-Mn forms a layered type-1 (CuAu type) antiferromagnetic phase which remains the ground state over a wide range of volumes.[28] Bcc δ-Mn shows a more complex behavior. The most recent *ab initio* calculations[28] predict a type-2 [(100) in-plane] AFM ground state, and a transition to layered type-1 ordering on expansion. Around the equilibrium density, a FM phase is intermediate in energy between type-2 and type-1 antiferromagnetism. Earlier studies[29,30] had ignored the possibility of type-2 antiferromagnetism, and therefore, ferromagnetism is often reported for δ-Mn in the literature. More complex ferrimagnetic[31] and helimagnetic[32] structures have also been investigated and found to be competitive in energy in the transition region between ferromagnetism and type-1 antiferromagnetism.

The magnetically induced tetragonal distortion of γ-Mn was first considered theoretically by Oguchi and Freeman,[33] finding excellent agreement with the measured axial ratio of Endoh and Ishikawa.[25] The tetragonal equilibrium states of Mn as a function of c/a have been investigated by Qiu *et al.*[30,34] using full-potential *ab initio* LSD calculations and by Krüger *et al.*[35] using a semiempirical *d*-band model. Qiu *et al.*[30] used the "experimental" atomic volume of 12.94 Å^3 estimated for γ-Mn by extrapolation from FeMn alloys[25] and compared only the FM and the layered AFM states. Antiferromagnetism was found to be preferred at all values of the axial ratio, the AFM energy vs c/a curve shows a stable tetragonal state at $c/a=0.96$ (close to the experimental value for γ-Mn) and a metastable distorted body-centered tetragonal state at $c/a=0.60$. In a subsequent calculation,[34] the constant volume constraint was relaxed, producing an equilibrium volume lower by nearly 10% than the measured value. Krüger *et al.*[35] used an empirical tight-binding Hamiltonian and compared four different types of AFM ordering: (i) type-1 (100) layer-by-layer ordering, (ii) type-2 in-plane ordering, and two further configurations which can be most easily considered as (110) and (011) layer-by-layer ordering (iii), (iv). At constant volume stability changes from in-plane (ii) to (110) layer-by-layer (iii) and to (100) layer-by-layer (i) with c/a increasing from the bcc to the fcc structure. This is an important result as it indicates that the AFM configuration is strongly dependent upon geometrical distortion, but quantitatively the result must be interpreted with some caution because of the empirical character of the Hamiltonian.

Krüger *et al.*[35] also examined the magnetic structure of the (100) surface of tetragonal Mn at atomic volumes and axial ratios considered to be representative for Mn/Fe(100) and Mn/Pd(100) (both intermediate between bcc and fcc Mn). Eight different configurations for the surface layer have been probed, but the magnetic order in the subsurface layers has been constrained to a (100) layer-by-layer ferrimagnetic configuration (allowing the magnitudes, but not the sign of the local magnetic moments to deviate from the bulk ordering). A $c(2\times2)$ AFM in-plane order with enhanced surface moments was found to represent the magnetic ground state of the surface in both cases. Previously, Aldén *et al.*[36] had calculated the magnetic contribution to the surface energy of the 3*d* metals, including γ-Mn and δ-Mn. It was found that magnetism strongly reduces the surface energy of open surfaces [i.e., of the (100) surfaces of the fcc and bcc structures], the effect being most pronounced for AFM Cr and Mn which show the by far most pronounced surface-induced enhancements of the magnetic moments.

Ultrathin films of Mn have been grown on a number of fcc (Al,[37] Cu, Ni,[38] Pd,[39] Ir[40]) and bcc Fe (Refs. 13 and 41) surfaces oriented in the [100] direction. In each case the Mn overlayers continue the square lattice of the substrate and adopt a strained face-centered tetragonal structure. As long as the growth conditions prevent interdiffusion, theoretical studies[18,42–46] and experiments agree on in-plane $c(2\times2)$ antiferromagnetism in the monolayer limit and layered antiferromagnetism in films with two and more monolayers. If Mn

is deposited at higher temperatures on late transition or noble metals (Cu, Ni, Ag, Pd),[47–51] ordered surface alloys with a $c(2\times2)$ structure are formed. Low-temperature phases show an irreversible phase transition on annealing, confirming the thermodynamic stability of the surface alloy. Surface alloying and the FM coupling between the Mn atoms in the alloy layers are confirmed by *ab initio* LSD calculations.[45,46]

Whereas for Mn grown on nonmagnetic substrates theory and experiment have converged to a rather clear picture of the structural and magnetic properties, experimental investigations and theoretical studies of Mn overlayers on Fe(100) have produced a wide range of conflicting results. Experiments have demonstrated that at low coverage Mn grows layer-by-layer, adopting a strained body-centered tetragonal structure in registry with the Fe substrate, changing to island growth beyond a critical thickness of the Mn film.[16,52–55] The estimates of the coverage at which the growth mode changes vary between three monolayers (ML) (Refs. 16 and 54) and 13 ML (Ref. 55). At still larger thickness, the tetragonal structure of the Mn film is possibly destabilized. Based on Mössbauer spectroscopy and reflection high-energy electron diffraction, Passamani *et al.*[56] suggested the presence of α-Mn at thicknesses above 10 Å. Earlier, Heinrich *et al.*[13] had reported formation of α-Mn and of a not completely identified, structurally related phase on a Ru substrate.

There are also considerable differences in the geometrical parameters (mainly the axial ratio of the tetragonal cell) and the degree of interdiffusion at the Fe/Mn interface. Whereas on the basis of Auger spectroscopy it was concluded[57] that already at moderate temperatures 60% of the deposited Mn undergo place exchanges with substrate atoms, scanning tunneling microscopy (STM) with chemical contrast[16] leads to an exchange rate of less than 20% at 370 K. Using photoelectron spectroscopy, Torelli *et al.*[58] detected the first signs of interdiffusion only at 450 K. Perhaps the most detailed view of the film structure is offered by STM measurements.[16,54] The Mn layers relax outward, and up to 4 ML the interlayer distances depend strongly on coverage, with a maximum of 1.8 Å at 3 ML. Beyond 4 ML the layer separation remains constant at 1.65 Å. Experimental estimates for the magnetic moment of the Mn atoms vary between $0.8\mu_B$ (Ref. 58) and $4.5\mu_B$ (Ref. 59), and other results cover the entire interval between these extremes ($1\mu_B$ of Ref. 60, $1.7\mu_B$ of Ref. 61, $3\mu_B$ of Ref. 41, $4\mu_B$ of Ref. 53). Even more controversial is the magnetic structure of the Mn film and its coupling to the Fe substrate, especially at low coverage. Three different scenarios have been advocated in the literature: (i) An in-plane AFM (or, more precisely, ferrimagnetic) Mn layer with two inequivalent Mn sites.[53,59,62] (ii) A layered antiferromagnetism in the Mn film with an antiferromagnetic coupling at the surface.[41,63] Alternatively, a ferromagnetic Fe/Mn coupling has been reported.[14] Very recent spin-polarized STM scans[17,64] suggested layered antiferromagnetism, but did not make a definitive conclusion as to the interface coupling. (iii) A FM Mn film coupled parallel to the substrate up to 2-3 ML, becoming AFM at higher coverages.[58,60,61]

The magnetic properties have been found to be extremely sensitive to surface contaminations. Andrieu *et al.*[65] have argued that a modest degree of oxidation of the Mn overlayer can reverse the sign of the Mn/Fe coupling at the interface.

Mn/Fe(100) is also a difficult case from a theoretical point of view. *Ab initio* investigations of isolated Mn atoms at Fe(100) surfaces[66,67] showed that a Mn adatom couples ferromagnetically and a Mn surface atom antiferromagnetically to the substrate. The exchange process between a Mn adatom and a Fe atom from the surface is exothermic, but Mn diffusion deeper into the surface is prevented by an exothermic segregation energy. Magnetism strongly reduces the exothermicity of the exchange process and drives the surface segregation.[67]

The magnetic structure of Mn monolayers on Fe(100) has been investigated using tight-binding[68,69] and *ab initio* LSD techniques,[42,70–73] allowing for a variety of spin structures. All calculations agree on a strongly enhanced surface moment ($>3\mu_B$) independent of the spin configuration. Wu and Freeman[42] suggested that the ground state of a Mn monolayer is $c(2\times2)$ AFM, driving a buckling reconstruction of the surface. Elmouhssine *et al.*[69] and Asada *et al.*[70] found the $c(2\times2)$ AFM configuration to be degenerate within a few meV/atom with a $p(2\times2)$ ferrimagnetic (FIM) state with three Mn atoms out of four coupling ferromagnetically and one atom antiferromagnetically to the substrate, but produced different signs for this modest energy difference. Both calculations neglect a possible relaxation or reconstruction of the surface and find a FM Mn layer coupling parallel to the surface to be disfavored only by a small magnetic energy difference [$\Delta E\approx50$ meV/Mn atom (Ref. 70)]. Only a few studies have considered higher Mn coverages, all implicitly assuming a (1×1) magnetic structure of the overlayer.[42,71,74] While Wu and Freeman[42] and Bouarab *et al.*[74] find that the addition of a second Mn layer does not disturb the FM Mn/Fe coupling at the interface, Mirbt *et al.*[71] reported that the magnetization of the outer Mn layer is parallel to that of the substrate, whereas the moments in the Mn interface are strongly quenched and aligned antiparallel to the substrate. This suggests that the orientation of the net magnetic moment of the overlayer relative to the film might be more important than the interface coupling.

Theoretical investigations of the magnetism of thicker Mn films have been published only very recently. Ernst *et al.*[75] used a Kohn-Korringa-Rostocker (KKR) Green's function approach to study layered antiferromagnetism in Mn films with up to 12 ML on a semi-infinite Fe(100) substrate. The KKR approach uses a muffin-tin potential, and a gradient-corrected exchange-correlation functional was used. The structure was assumed to be body-centered tetragonal, with the in-plane lattice constant fixed to the experimental value for α-Fe and the interlayer distances in the Mn film adjusted to the experimental values reported by Yamada *et al.*[16] No relaxation was allowed. The calculations used a $p(1\times1)$ surface cell and assumed alternating signs of the magnetic moments in subsequent Mn planes, i.e., only layered AFM solutions were permitted. Antiferromagnetic coupling at the Mn/Fe interface and strongly enhanced Mn surface moments were reported. Surprisingly the calculations show a rather strong bias of the magnetic moments in the near-surface layers in the direction of the moment at the free surface. So far such a bias was not observed in any other *ab initio* calcula-

tion of magnetic thin films. Martinez *et al.*[76] investigated 6- and 7-ML-thick films using a tight-binding linear-muffin-tin orbital approach. The geometric setup of the model is very similar to that used by Ernst *et al.* (same in-plane lattice constant, Mn-Mn interlayer distances taken from experiment[16]), $p(1\times1)$ surface cell. Several collinear magnetic configurations were found, with only small magnetic energy differences which reveal a competition between FM and layered AFM ordering. The most stable configurations show layer-by-layer AFM in the Mn film, with a ferromagnetic Mn/Fe coupling at the interface. Also most metastable configurations show a FM interface coupling, only for the 6 ML film a layered AFM configuration with an AFM interface coupling is reported—but this configuration is the least favorable in energy. While Ernst *et al.*[75] report "that Fe electronic states do not hybridize significantly with Mn states," Martinez *et al.*[76] note a pronounced Fe-Mn hybridization (as one would intuitively expect, given the broad overlap of the *d* bands of both metals). The striking differences between these recent investigations underline the difficulties of achieving a correct description of this system.

Despite the evident importance for understanding the properties of Mn/Fe(100) films, systematic investigations of surface alloying are very scarce. Torelli *et al.*[58] performed Monte Carlo studies based on an embedded atom model (i.e., disregarding magnetic effects) and found that the surface alloying is a moderately exothermic, activated process with an activation energy of about 1.3 eV. Taguchi *et al.*[77] used *ab initio* LSD methods to compare the total energies of an ideal $c(2\times2)$ AFM overlayer and an ordered FeMn bilayer with FM in-plane and AFM interlayer coupling and reported an energy difference of only 7 meV/Mn atom in favor of the alloyed surface.

The properties of Fe/Mn/Fe sandwich structures are even more complex. While earlier investigations[78] reported a two-ML oscillation in the AFM exchange coupling through Mn in Fe/Mn/Fe sandwiches, recent studies[14,15,79,80] agree on a FM coupling through ultrathin Mn spacers (up to 4 ML) and a noncollinear coupling for thicker spacers, with a canted FM state between 4 and 8 ML, and oscillations of the coupling angle between $90°+\phi$ and $90°-\phi$ beyond 9 ML, ϕ varying between 10° and 30°, depending on sample preparation. It has been argued that the noncollinear coupling is better explained by the proximity model of Slonczewski[81] than by a bilinear-biquadratic coupling model. Since within the proximity model a noncollinear coupling appears only for a rough interface, this would explain that the critical thickness for the onset of noncollinearity coincides with the change of the growth morphology from layer-by-layer to layer plus islands. However, in view of the results discussed above, it cannot be taken for granted that the basic assumption of the proximity model (strong short-range coupling at the interface) is really fulfilled in Fe/Mn/Fe sandwiches.

In this work we present a detailed investigation of the structural and magnetic properties of tetragonal Mn in the bulk, at a Mn(100) surface, and in ultrathin Mn films grown on a Fe(100) substrate. Our studies are based on local spin-density theory (using gradient-corrected exchange-correlation functionals) and concentrate on the cross-correlations between the geometric and magnetic structures. Collinear as well as noncollinear magnetic ordering is considered.

II. METHODOLOGY

All calculations reported here were performed within the framework of density functional theory. We used the Vienna *ab initio* Simulation Package (VASP) (Ref. 82) and employed the projector augmented-wave (PAW) potentials[83,84] supplied with the code. Exchange and correlation effects were described by the energy functional parameterized according to Perdew and Zunger[85] employing the spin interpolation proposed by Vosko *et al.*[86] and adding generalized gradient corrections.[87] Earlier calculations[45,88] have demonstrated that the use of the generalized gradient approximation (GGA) is mandatory for magnetic Mn, as the local density approximation predicts a nonmagnetic hexagonally close-packed ground state for Mn (and also for Fe), whereas the GGA leads to correct structural and magnetic energy differences for all Mn polymorphs.[27,28] The cutoff energy for the plane-wave basis construction was set to 300 eV. For both iron and manganese 3*d* and 4*s* states were treated as valence states. The lattice parameter calculated for iron, $a_{\mathrm{Fe}}=2.83$ Å is by 1% lower than the measured value. The structural parameters of manganese in its various phases will be presented below.

Most calculations assumed a collinear magnetic structure and were performed in a scalar-relativistic mode. For bulk Mn we also investigated long-period helical magnetic structures, using an approach pioneered by Herring[89] and implemented in VASP by Marsman[90] on the basis of the unconstrained vector-field description of the magnetization density developed by Hobbs *et al.*[91] For Mn/Fe(100) we investigated also noncollinear magnetic configurations using the same vector-field description. Because of the possible influence of the magnetic anisotropy, these calculations were performed in a fully relativistic mode, including spin-orbit coupling.

Local densities of states and the atomic magnetic moments were calculated by projection of the plane-wave components of the eigenstates onto spherical harmonics centered around atoms. The sphere radii were 1.22 Å for both iron and manganese, corresponding to touching spheres in bulk iron. Surfaces and thin films were modeled by periodically repeated slabs. The details of the slab construction will be given separately in the corresponding sections below as they differ for compact and surface structures. The actual number of *k* points used in the integrations over the Brillouin zone depends on the slab size and symmetry, and it will also be specified separately for each model later. In order to facilitate convergence of the calculations, the eigenvalues were smeared using the Methfessel-Paxton method[92] with a smearing parameter of 0.2 eV. The smearing leads to a partial occupation of electron orbitals close to the Fermi energy, improving convergence especially for metallic systems.

In the plane-wave based codes it is fairly easy to calculate the forces acting on the atoms and the stresses on the unit cell. Structural optimizations have been performed by adjusting the cell parameters and moving the atoms according to the stresses and forces until the total-energy minimum is

reached. We have performed such a structural optimization for the tetragonal bulk phases and for surfaces and thin films (with fixed in-plane lattice constants) using a quasi-Newton algorithm. The criterion for stopping the ionic relaxation was a convergence of the interatomic forces within 10 meV/Å.

III. TETRAGONAL Mn BULK AND SURFACE

We begin by discussing the intrinsic magnetic properties of tetragonal Mn in the bulk and on the (100) surface. In addition to the nonmagnetic and the FM configurations, we considered three different AFM phases: (i) layered antiferromagnetism in (100) planes (equivalent to CsCl-type and CuAu-type AFM in the bcc and fcc structures, respectively), (ii) bilayer antiferromagnetism, and (iii) in-plane $c(2\times2)$ antiferromagnetism. These magnetic configurations have also been considered in our studies of Mn surfaces. For bulk tetragonal Mn, we examined in addition the possibility of the formation of noncollinear helical spin structures.

A. Magnetism of the strained tetragonal Mn-collinear case

The structural models for tetragonal Mn consist of two planes perpendicular to the (100) direction, each accommodating two atoms, only for the bilayer AFM configuration models with four planes and one atom per plane were used. The total energy $E(a,c/a)$ was evaluated as a function of the in-plane lattice constant a in the range between 3.35–4.16 Å with a step of 0.015 Å, and as a function of an axial ratio c/a ranging from 0.62 to 1.20 with an increment of 0.02. k-space integration was performed on a grid of $14\times14\times14$ points.

Figure 1 summarizes our results for the total energy, magnetic moment, and equilibrium atomic volume of all five magnetic configurations of tetragonally strained Mn as a function of the axial ratio. Three locally stable states have been identified: (i) A layer AFM phase with a distorted fcc structure, axial ratio $c/a=0.945$, an in-plane lattice constant $a=3.632$ Å (corresponding to an atomic volume $V_{\mathrm{at}}=11.32$ Å^3) and a magnetic moment $m=1.77\mu_B$. (ii) An in-plane $c(2\times2)$ AFM phase with a distorted fcc structure, axial ratio $c/a=1.049$, an in-plane lattice constant $a=3.506$ Å (corresponding to an atomic volume $V_{\mathrm{at}}=11.30$ Å^3) and magnetic moment $m=1.75\mu_B$. The energy difference between these two AFM states is only 6 meV/atom, both have almost the same atomic volume and magnetic moment. This result demonstrates an extreme sensitivity of the AFM order to even small variations of the tetragonal strain. (iii) A second local minimum for an in-plane AFM phase is found for a slightly distorted bcc structure [axial ratio $c/a=0.684$, compared to $c/a(\mathrm{bcc})=0.707$]. The in-plane lattice constant is $a=4.023$ Å^3, the atomic volume $V_{\mathrm{at}}=11.13$ Å^3 is slightly lower than for the nearly fcc phases. The magnetic moment is $m=1.42\mu_B$, the energy difference relative to the layered AFM phase with $c/a=0.945$ is 81 meV/atom.

While an in-plane AFM solution exists over the entire range of c/a, the layered AFM state is unstable for nearly bcc structures. Vice-versa, a metastable FM solution with magnetic moments less than $1\mu_B$ exists only for slightly distorted bcc lattices. A bilayer AFM solution exists only for compressed bcc structures. Up to an axial ratio of $c/a=0.821$ the magnetic ground-state configuration is in-plane AFM, with a magnetic moment of about $1.5\mu_B$ and an equilibrium atomic volume varying only between 11.10 and 11.33 Å^3. Between $c/a=0.821$ and $c/a=1.0$ the ground state is layered (100) AFM, with a magnetic moment that slowly increases from 1.5 to $1.8\mu_B$ and an atomic volume of 11.15 to 11.31 Å^3. For the undistorted fcc phase with $c/a=1.0$ the in-plane and layer AFM phases are merely two alternate descriptions of the same magnetic structure. For $c/a>1.0$ the ground state is again in-plane AFM, $m=1.55$ to $1.74\mu_B$, $V_{\mathrm{at}}=11.17$ to 11.30 Å^3. Independent of the axial ratio, a strong magnetovolume effect is predicted because the equilibrium volume of nonmagnetic tetragonal Mn is near 10.7 Å^3 throughout.

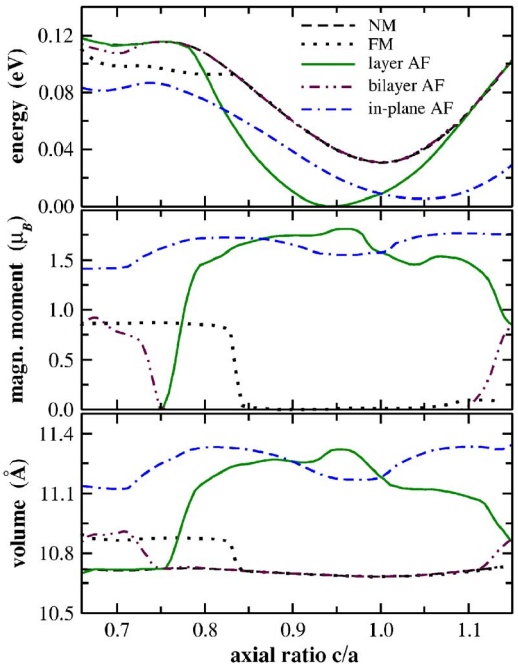

FIG. 1. (Color online) Total energy, magnetic moment, and atomic volume as a function of the axial ratio for five different magnetic phases of tetragonal Mn. All plotted values are obtained for the equilibrium lattice constant a found separately for each c/a ratio.

Because in the following we are going to explore properties of Mn films grown on Fe(100) surface, it is instructive to look more closely on bulk Mn with the lattice constant in the (100) plane constrained to that of bcc Fe. If the in-plane lattice constant is adjusted to the lattice parameter of bcc Fe [$a_{\mathrm{Fe}}=2.83$ Å, corresponding to $a_{\mathrm{Fe}}(\mathrm{fcc})=4.00$ Å] while axial ratio and atomic volume are allowed to relax, the ground state is in-plane AFM with $c/a=0.694$, $V_{\mathrm{at}}=11.12$ Å^3, and $m=1.42\mu_B$. Layered AFM is unstable, it relaxes to a nonmagnetic state with $c/a=0.669$, $V_{\mathrm{at}}=10.72$ Å^3 and a magnetic energy difference of 36 meV/atom. A FM state is only 20 meV/atom above the ground state, with $c/a=0.678$, $V_{\mathrm{at}}=10.86$ Å^3, and $m=0.86\mu_B$. A bilayer AFM phase is metastable with an energy higher by 28 meV/atom than in the ground state, $c/a=0.683$, $V_{\mathrm{at}}=10.94$ Å^3, and $m=0.88\mu_B$.

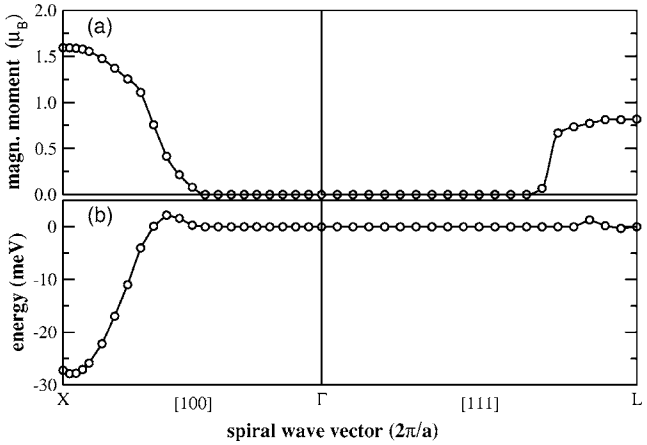

FIG. 2. Magnetic moment (a) and total energy (b) of spin-spiral states in cubic γ-Mn with $a=3.542$ Å for spiral wave vectors along the $\overline{\Gamma X}$ and $\overline{\Gamma L}$ directions.

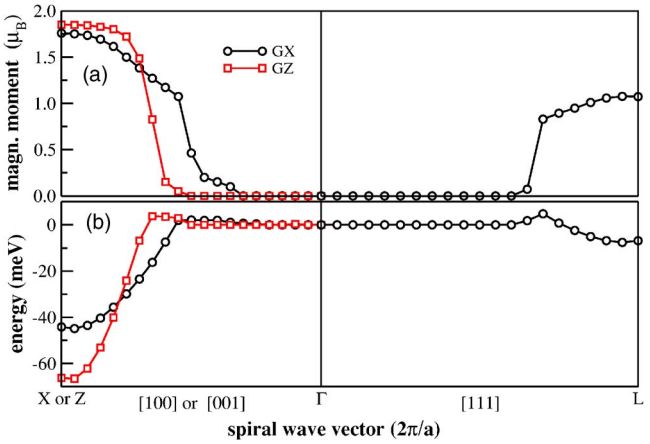

FIG. 3. (Color online) Magnetic moment (a) and total energy (b) of spin-spiral states in tetragonal γ-Mn with $a=3.542$ Å, $c/a=0.945$, for spiral wave vectors along the $\overline{\Gamma X}$, $\overline{\Gamma Z}$, and $\overline{\Gamma L}$ directions. See text.

These results are remarkable in two respects. First, they demonstrate a pronounced tendency to conserve the atomic volume characteristic of the magnetic phase, independent of the strength of the tetragonal distortion. Second, they suggest that Mn films stabilized by epitaxial growth on bcc Fe will come very close to bcc δ-Mn and eventually adopt an in-plane AFM state, in contrast to the layered AFM configuration postulated in the literature which we find to be unstable. However, as already suggested in the literature, the ground state of δ-Mn is not necessarily collinear. Our results for the tetragonal bulk phase of Mn differ considerably from those of Qiu *et al.*,[30,34] who considered only the layered AFM phase, but have not included the possibility of in-plane magnetic ordering. Qiu *et al.* reported a metastable layered AFM minimum at $c/a \approx 0.6$, but failed to report any information on the magnetic moments. Our calculations show that magnetism has already disappeared for such large tetragonal strains, if only layered AFM ordering is admitted. Even larger differences exist with the KKR calculations of Ernst *et al.*[75], who reported a magnetic moment as large as $2.3\mu_B$ for tetragonally expanded body-centred Mn ($c/a=1.14$)—such large moments had never been reported for δ-Mn in any previous calculation (see Hobbs *et al.*[28] for detailed references to earlier work).

B. Magnetism of the strained tetragonal Mn-noncollinear case

Motivated by the earlier work of Mohn *et al.*[32] on helical magnetism in δ-Mn, we have explored the possibility of incommensurate spin-spiral states in γ- and δ-Mn. VASP allows one to perform calculations for long-period helical magnetic structures based on the crystallographic unit cell only,[89,90] but it requires very high accuracy of the Brillouin-zone integrations. In these calculations with a unit cell containing only a single atom we have employed 2197 k points (a $13\times13\times13$ grid) distributed over the whole Brillouin zone. Additional calculations performed with 4913 k points in order to check the convergence of the total energy differed at most by 0.3 meV. Our results are compiled in Figs. 2–4. For ideal fcc Mn we find that spin-spiral solutions exist only in the vicinity of the X and L point. The X point corresponds to the layered (100) AFM solution, the L point to a stacking of ferromagnetic layers with alternating signs of the moments along the [111] direction (which is higher in energy by about 30 meV and has a magnetic moment of $0.8\mu_B$, see Fig. 2). For shorter spiral wave vectors magnetism breaks down, reflecting the instability of the FM solution noted above.

The results for spin-spiral states in tetragonally distorted γ-Mn ($c/a=0.945$) are summarized in Fig. 3. The degeneracy of helical states with wave vectors along the [100] and [001] directions is lifted, and a layer AFM structure along the tetragonal axis is found to be energetically favored. Interestingly, the total energy minimum is found not exactly at the Z point, but for a wave vector $\vec{q}_{\min}=0.985\times(2\pi/c)[001]$. The energy difference is minimal, but we have checked very carefully that this result, which indicates a possible formation of a long-period magnetic superstructure, is independent of the computational setup.

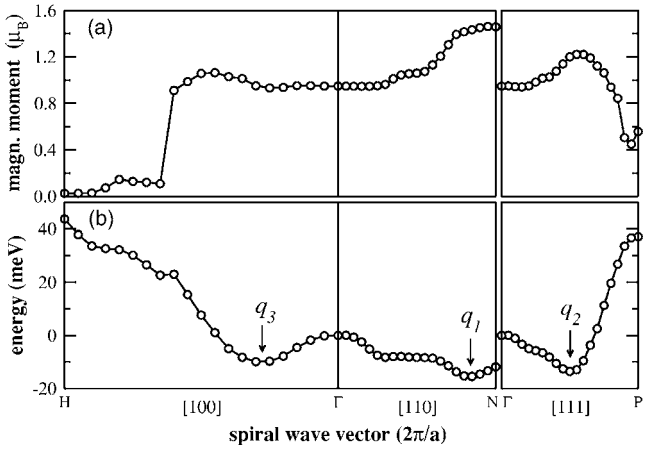

FIG. 4. Magnetic moment (a) and total energy (b) of spin-spiral states in cubic δ-Mn (bcc) with $a=2.815$ Å for spiral wave vectors along the high-symmetry directions. Note the existence of noncollinear phases (indicated by the spin-spiral wave vectors q_i) with a lower energy than the collinear in-plane AFM state.

TABLE I. Layer-resolved magnetic moments m_i (in μ_B), interlayer relaxations $\Delta_{i,i+1}$ (in percent of the bulk interlayer distance $c/2$) and surface energy σ (in eV/surface atom) for the (100) surfaces of the locally stable phases of tetragonal Mn. The solution denoted as IV is related to the solution I, but here the moments within the topmost layer are antiparallel.

	I a=3.632 Å c/a=0.945 layered AFM σ=1.16		II a=3.506 Å c/a=1.049 in-plane AFM σ=1.10		III a=4.032 Å c/a=0.684 in-plane AFM σ=1.03		IV a=3.632 Å c/a=0.945 in-plane AFM on surface layered AFM in bulk σ=1.06	
i	m_i	$\Delta_{i,i+1}$	m_i	$\Delta_{i,i+1}$	m_i	$\Delta_{i,i+1}$	m_i	$\Delta_{i,i+1}$
1	−2.87	−1.5	±2.71	−0.2	±3.52	10.0	3.26/−2.95	11.2/−4.6
2	1.70	−0.8	±1.39	−3.4	±0.30	−7.8	1.54/1.54	−0.7/−0.7
3	−1.68	−0.5	±1.59	0.7	±1.69	12.5	−1.53/−1.82	−1.3/0.1
4	1.75	0.5	±1.81	0.9	±1.30	−8.4	1.72/1.72	0.1/0.1
5	−1.80	0.4	±1.76	−0.1	±1.22	10.6	−1.77/−1.77	0.2/0.2
6	1.79	0.2	±1.72	0.3	±1.82	−5.4	1.75/1.75	0.0/0.0
bulk	±1.80	1.716[a]	±1.74	1.839[a]	±1.42	1.376[a]	±1.80	1.716[a]

[a]Interlayer distance in the bulk, in Å.

The analysis of spin-spiral states in bcc δ-Mn leads to very interesting results. In analogy to the earlier study by Mohn *et al.*[32] we find multiple local minima representing metastable spin-spiral states. Our results for wave vectors along the [100], [110], and [111] directions are summarized in Fig. 4. In these graphs the H point represents the layered (100) AFM state, the N point the $c(2\times2)$ in-plane AFM phase, the P point a third AFM phase with alternating moments in planes stacked along the [111] direction, and the Γ point the FM phase. This third AFM configuration and the FM phase are found to be unstable against a long-period modulation of the magnetic structure. The energetically most favorable collinear phase at the N point does not represent the absolute minimum—it is unstable against a modulation with a wave vector $\vec{q}_1=0.843\times(2\pi/a)[110]$, the magnetic energy difference is about 4 meV. A slightly shallower minimum which is also more favorable than the collinear state is located exactly halfway between the Γ and P points, at $\vec{q}_2=0.5\times(2\pi/a)[111]$. In this configuration, the magnetic moments in successive (111) planes are rotated by 90°. In both noncollinear states the magnetic moment is a bit smaller than in the collinear phase. The third local minimum, slightly higher in energy than the collinear ground state, is located at $\vec{q}_3=0.27\times(2\pi/a)[100]$, representing, like the absolute minimum at $\vec{q}_1$, an incommensurate spin-spiral.

Altogether these results demonstrate that tetragonal Mn has an extremely rich magnetic phase diagram. Of course, the stable magnetic structure will strongly vary with the tetragonal strain, with noncollinear solutions also for distorted bcc structures. However, investigation of these phases goes beyond the scope of the present work.

C. Structure and magnetism of the (100) surface of tetragonal Mn

The structure and magnetic properties of the (100) surfaces for the three locally stable phases of tetragonal Mn have been examined using calculations on periodically repeated slabs. We have used slabs consisting of ten Mn layers (the lowest four ML are fixed in a bulklike geometry) and a $c(2\times2)$ surface cell to enable a comparison of in-plane and layered AFM phases. Adjacent slabs are separated by a vacuum region of about 15 Å. A $(9\times9\times1)$ grid of k points was used, leading to 15 up to 25 k points, depending on the magnetic symmetry of the model.

The characteristic properties of the Mn surfaces are a strong enhancement of the magnetic moment in the surface layer, decaying in an oscillatory way toward the bulk value in the deeper layers, and an oscillatory relaxation of the interlayer distances. This requires the use of rather thick slabs—for the nearly fcc configurations, interlayer relaxations are modest (see Table I) and the oscillations in the layer-resolved magnetic moments are well converged with respect to slab thickness. For both the contracted layered AFM phase (c/a=0.945) and for the expanded in-plane AFM phase (c/a=1.049) we find a strong enhancement of the surface magnetic moments to about $2.8\mu_B$ and a weak inward relaxation of the topmost layer. The surface-induced enhancement of magnetism is almost independent of the surface relaxation, only the variation of the moments in the subsurface layers is somewhat dependent on the variation of the interlayer distances.

A much stronger surface relaxation is predicted for the nearly bcc (c/a=0.684) in-plane AFM phase. Here we find alternating expansions and contractions of the interlayer distances by about ±10%, coupled to a very pronounced enhancement of the surface moments to $3.5\mu_B$, a strong quenching of magnetic moments in the subsurface layer to $0.3\mu_B$, followed by an oscillatory convergence towards the bulk value. Admittedly, to achieve complete convergence of the moments and layer spacings to their respective bulk values, calculations based on even thicker slabs (which are hard to converge because of charge-sloshing problems) would be

required. However, comparison with calculations based on 6-ML slabs make us confident that the results given in Table I are at least semiquantitatively reliable.

The comparison of the surface energies leads to a notable result. The lowest surface energy of $\sigma=1.028$ eV/atom ($=2.68$ J/m^2) is found for the nearly bcc phase with in-plane AFM, which shows the strongest surface-induced enhancement of magnetism and the most pronounced vertical relaxations. Also, for the nearly fcc phase, the one expanded along the tetragonal axis and in-plane AFM has a lower surface energy than the compressed phase with in-plane AFM. For these two phases, the difference in the surface energies ($\Delta\sigma=65$ meV/atom) is even larger than the structural and magnetic energy difference in the bulk ($\Delta E=54$ meV/atom). This result motivated us to investigate the possibility of the formation of an in-plane ordered surface on top of a layered AFM bulk.

If the magnetic moments in the surface layer of tetragonally contracted near fcc Mn are initialized in a $c(2\times2)$ AFM structure, with layered AFM in the deeper region, the final result is a $c(2\times2)$ ferrimagnetic surface layer with magnetic moments of $+3.26\mu_B$ and $-2.95\mu_B$ and a pronounced buckling. The Mn atom carrying the larger moment and coupling ferromagnetically to the subsurface layer relaxes outward by 11.2%, whereas the atom with an antiferromagnetically coupled moment relaxes inward by −4.6%. The buckling also extends to the second subsurface layer in which the atoms are straight below the surface atoms. Due to the long-range exchange coupling, the magnetic moments in this layer also differ by $0.3\mu_B$. The most important result, however, is that the formation of an in-plane AFM surface layer lowers the total energy of the slab by 95 meV/surface atom, as anticipated from the difference in the surface energies. This result suggests that not only for monolayer, but also for thicker Mn films, the possibility of an in-plane antiferromagnetism cannot be dismissed *a priori*.

IV. ULTRATHIN Mn FILMS ON Fe(100) SUBSTRATES

A. Submonolayer coverage

The energetics and the magnetic coupling of Mn adatoms and surface impurities have already been explored by earlier *ab initio* calculations. According to Nonas *et al.*,[67] a Mn adatom couples ferromagnetically to surface, while a surface impurity couples antiferromagnetically. The exchange process between an adatom and a substrate atom is an exothermic process with a heat of reaction about −0.3 eV if a transition from a FM adatom to a FM surface impurity is considered, and about −0.6 eV if the exchange process is coupled to a reorientation of the Mn moment.

Here we are interested mainly in the magnetic structure of Mn overlayers at submonolayer coverage. We investigated Mn films with a coverage of 0.25 ML, using slabs consisting of six Fe ML and a (4×4) surface cell. The Mn atoms are either distributed homogeneously over the surface or arranged in compact square 2×2 clusters. For the clusters we examined a FM Mn-Mn interaction together with a FM or AFM coupling to the Fe substrate, and an AFM Mn-Mn interaction, leading to a magnetic structure related to a fragment of the $c(2\times2)$ in-plane AFM configuration. This last configuration turned out to represent the ground state with Mn moments of $-3.61\mu_B$ and $3.45\mu_B$ and a slight buckling of 0.14 Å (Mn atoms coupling ferromagnetically to the surface are located higher above the surface). A FM cluster ($m_{\mathrm{Mn}}=3.63\mu_B$) coupling ferromagnetically to the substrate has an energy higher by 11 meV/Mn atom, antiferromagnetic coupling at the Mn/Fe interface leads to an energy difference of 77 meV ($m_{\mathrm{Mn}}=3.48\mu_B$).

A homogeneous distribution of the Mn atoms over the Fe surface in a $p(2\times2)$ checkerboard pattern leads to a substantially higher energy. The energetically most favorable solution (but still higher by $\Delta E=406$ meV/Mn atom than the clustered ground state) is found for a FM Mn overlayer coupling AFM to the Fe substrate ($m_{\mathrm{Mn}}=-3.57\mu_B$). AFM in-plane ordering in the Mn adlayer ($m_{\mathrm{Mn}}=+3.72\mu_B$ and $-3.59\mu_B$) increases the total energy by an additional 64 meV/Mn atom, FM interface coupling of a FM adlayer ($m_{\mathrm{Mn}}=3.71\mu_B$) by an additional 106 meV/Mn atom.

These results demonstrate the following. (i) A very strong attractive interaction between the adatoms leads to the formation of Mn islands. The energy gain by the lateral interactions is of the same order as the exchange energy between a Mn atom and a substrate atom. (ii) Within the clusters, a change from in-plane AFM to FM order costs considerably less energy than the reversal of the favored FM interface coupling into AFM coupling. (iii) For a homogeneously distributed submonolayer film (which will be formed only if island formation is diffusion limited) the coupling between third nearest-neighbor Mn atoms is FM, but the interface coupling is AFM. This observation could explain why both FM and AFM interface coupling has been reported in experimental studies of submonolayer Mn films.

B. Structure and magnetism of epitaxial Mn/Fe(100) films with 1 to 6 monolayers—collinear case

Mn/Fe(100) films were simulated by two types of slabs, one with a (1×1) surface periodicity used for layered magnetic structures and the second one with a (2×2) surface periodicity suitable for in-plane AFM structures. In both cases the iron substrate is modeled by six layers. In the former case k-space sampling is performed using a grid of $(15\times15\times1)$ points, in the latter case a grid of $(10\times10\times1)$ was employed.

In Table II we have compiled our results for the geometric and magnetic properties of ultrathin Mn overlayers epitaxially grown on Fe(100). We have examined different magnetic configurations: (i) a sequence of layered (A)FM configurations—in principle, for a film consisting of n monolayers, there are 2^n different ways to align the spins in the successive Mn layers, and (ii) in-plane $c(2\times2)$ antiferromagnetism in the surface layer followed by layered AFM ordering. The magnetic moments in the deeper layers are allowed to relax to the ground state. The calculations for the layered configurations were first performed using (1×1) surface cells. For the most stable layered configuration the calculation was repeated using a $c(2\times2)$ surface cell to allow

TABLE II. Magnetic moments m_i (in μ_B), interlayer relaxations $\Delta_{i,i+1}$ (in per cent of the interlayer distance in bulk bcc Fe, d=1.415 Å), and energy differences ΔE (in meV/Mn atom) for various magnetic configurations of Mn/Fe(100) films. The magnetic structure of the Mn is described by the labels u (upwards, i.e., parallel to the substrate moments) and d (downwards, i.e., antiparallel to the substrate moments) for layer AFM, $c(2\times2)$ stands for in-plane AFM in the topmost Mn layer.

	1-ML Mn/Fe(100)					
	$c(2\times2)$		Fe|u		Fe|d	
	m_i	$\Delta_{i,i+1}$	m_i	$\Delta_{i,i+1}$	m_i	$\Delta_{i,i+1}$
Mn	3.32/−3.59	3.7/1.3	3.50	6.3	−3.34	−2.7
Fe	1.42/1.57	−2.2/−2.2	1.75	−3.1	1.76	2.4
Fe	2.30/2.30	2.9/−0.5	2.10	1.0	2.46	0.0
ΔE	0		34		170	

	2-ML Mn/Fe(100)							
	$c(2\times2)$		Fe|ud		Fe|du		Fe|dd	
	m_i	$\Delta_{i,i+1}$	m_i	$\Delta_{i,i+1}$	m_i	$\Delta_{i,i+1}$	m_i	$\Delta_{i,i+1}$
Mn	3.50/−3.48	7.1/9.0	−3.21	−7.1	3.44	2.9	−3.63	15.4
Mn	0.08/−0.70	−6.1/−6.3	1.75	7.4	−0.34	−0.5	−1.75	−8.1
Fe	2.05/1.89	2.0/2.2	2.33	−1.0	2.24	1.0	1.99	3.2
Fe	2.35/2.35	−0.3/−0.5	2.21	0.7	2.31	−0.4	2.40	−0.5
ΔE	0		12		32		103	

	3-ML Mn/Fe(100)									
	$c(2\times2)$		Fe|udd		Fe|dud		Fe|ddu		Fe|udu	
	m_i	$\Delta_{i,i+1}$	m_i	$\Delta_{i,i+1}$	m_i	$\Delta_{i,i+1}$	m_i	$\Delta_{i,i+1}$	m_i	$\Delta_{i,i+1}$
Mn	−3.51/3.59	9.4/9.7	−3.62	13.9	−3.45	2.3	0.34	−29.0	3.52	5.6
Mn	−0.63/−0.63	−11.0/−11.0	−1.17	−11.7	0.47	2.6	−0.28	6.1	−0.84	−2.7
Mn	0.45/1.76	4.8/6.2	1.55	5.3	−2.18	−3.2	−0.02	−4.8	2.06	3.2
Fe	2.30/2.30	−0.7/−0.7	2.26	−1.3	1.89	−0.6	2.01	1.5	2.06	−3.5
Fe	2.29/2.26	1.0/1.0	2.25	1.3	2.39	1.0	2.31	−0.6	2.17	−0.8
ΔE	0		32		90		162		214	

	4-ML Mn/Fe(100)					
	$c(2\times2)$		Fe|$uddu$		Fe|$udud$	
	m_i	$\Delta_{i,i+1}$	m_i	$\Delta_{i,i+1}$	m_i	$\Delta_{i,i+1}$
Mn	−3.38/3.57	4.4/9.8	3.15	−7.8	−3.44	2.7
Mn	−0.20/−0.20	−9.2/−9.3	−1.95	15.9	0.58	3.8
Mn	−0.76/1.44	0.2/7.6	−1.74	−12.9	−1.10	−6.3
Mn	1.78/1.77	−1.3/−1.4	1.62	6.1	1.96	2.8
Fe	1.96/1.87	−1.2/1.3	2.23	−1.5	2.15	−1.4
Fe	2.28/2.28	0.6/0.6	2.21	0.9	2.24	0.6
ΔE	0		11		25	

	5-ML Mn/Fe(100)							
	$c(2\times2)$		Fe|$uddud$		Fe|$udduu$		Fe|$uduuu$	
	m_i	$\Delta_{i,i+1}$	m_i	$\Delta_{i,i+1}$	m_i	$\Delta_{i,i+1}$	m_i	$\Delta_{i,i+1}$
Mn	3.58/−3.60	11.5/9.5	−3.57	6.7	3.65	15.1	3.66	10.9
Mn	0.61/0.61	−12.2/−12.2	0.65	−3.7	1.16	−13.1	0.07	−11.3
Mn	−0.71/−1.86	10.5/10.5	−2.23	10.8	−1.71	12.7	0.56	9.1
Mn	−1.68/−1.68	−12.4/−12.4	−1.40	−14.0	−1.80	−13.3	−0.38	−12.2
Mn	1.69/1.54	5.7/5.7	1.39	5.4	1.51	5.7	1.35	4.1
Fe	2.25/2.25	−1.4/−1.4	2.22	−1.7	2.25	−1.7	2.23	−0.5
Fe	2.24/2.24	1.1/1.1	2.22	0.9	2.23	0.7	2.30	1.4
ΔE	0		17		19		54	

for a comparison of the total energy for layered and in-plane configurations.

For a single Mn layer FM coupling to the substrate is favored over AFM coupling, but in-plane antiferromagnetism was found to be even lower in energy. In all three configurations, the size of Mn moments is about $3.5\mu_B$, Fe moments at the interface are reduced to values that are lower than in bulk Fe. In the $c(2\times2)$ phase, the Mn moments oriented oppositely to the surface are slightly larger ($-3.59\mu_B$) than those coupled ferromagnetically to the surface ($3.32\mu_B$). Hence this phase is sometimes also called ferrimagnetic. The Mn layer is slightly corrugated, with ferromagnetically aligned Mn atoms showing more outward relaxation. The preference for in-plane AFM order in the Mn/Fe(100) monolayer agrees with earlier *ab initio* calculations.[42,70–72]

For a bilayer we have tested all four possible layered magnetic configurations: Fe$|uu$, Fe$|ud$, Fe$|du$, Fe$|dd$ (u = spin up, i.e., parallel to the moments in the substrate, d = spin down). An initially completely FM configuration (Fe$|uu$) converged to Fe$|du$, all other layered configurations are at least metastable. The lowest energy was found for Fe$|ud$, followed by Fe$|du$ and Fe$|dd$. Our result for the most favorable layered magnetic configuration agrees with the conclusions of Wu and Freeman,[42] but disagrees with Mirbt *et al.*[71] and Asada *et al.*[72], who found the Fe$|du$ configuration with an almost completely quenched Mn interface moment to be lower in energy by about 9 meV/Mn atom. Clearly the discrepancy is to be attributed to the neglect of interlayer relaxations in these studies, as we find completely different relaxation patterns in all three configurations. In the stable Fe$|ud$ phase, the distance between the AFM coupled Mn layers shrinks by −7% compared to the substrate, whereas the Fe-Mn distance at the interface is expanded by a nearly equal amount; in the Fe$|du$ phase the Mn-Mn distance expands by 3% and there is almost no change in the interlayer distance at the interface. The Fe$|du$ configuration is energetically preferred if relaxation is suppressed.

The true magnetic ground state, however, shows $c(2\times2)$ in-plane AFM in the surface layer with large moments of $3.50\mu_B$ and $-3.48\mu_B$ (i.e., almost complete magnetic compensation), while the Mn interface layer is ferrimagnetic with strongly quenched moments of $-0.70\mu_B$ and $+0.08\mu_B$. The relaxation pattern of the $c(2\times2)$ surface is just opposite to that of the layered Fe$|ud$ phase: the Mn-Mn distance is expanded, the Fe-Mn distance contracted, both by about 7% (see Table II). Again the strong dependence of the film structure on the magnetic order explains the reversed stability of layered and in-plane configurations compared to Asada *et al.*[72] in whose calculations relaxation has been neglected.

For a 3-ML Mn/Fe(100) film there are eight distinct layered magnetic configurations. Three of these are found to be unstable: the FM configuration Fe$|uuu$ converged to Fe$|dud$, Fe$|ddu$ to Fe$|udu$, and Fe$|duu$ to Fe$|udu$. Our results for the remaining phases are listed in Table II. The most stable layered phase is Fe$|udd$, with a FM Mn/Fe coupling at the interface and a FM Mn bilayer at the free surface. In the bilayer the surface moment is enhanced to $3.6\mu_B$, whereas in the subsurface layer the Mn moment is reduced to $1.17\mu_B$, i.e., smaller than the moment in bulk δ-Mn. Interestingly, the interface moments of both Fe and Mn are very close to their bulk values. The Mn-Mn interlayer distance is strongly expanded between FM coupled layers and contracted if the coupling is AFM. However, in-plane AFM order in the surface layer leads to a lower total energy ($\Delta E=32$ meV/Mn). Alignment of the Mn moments in the deeper Mn layers is always parallel. In the subsurface layer the magnetic moments are strongly quenched, but equal by symmetry. In the interface layer, where the atomic positions of Mn are in registry with those in the surface layer, the FM Mn/Fe coupling enforces an up orientation of all Mn moments, but the moment of the Mn atom coupling to the negative surface moment is strongly reduced to $0.45\mu_B$ because at these distances Mn atoms couple ferromagnetically. Again, one finds a strong oscillatory interlayer relaxation, following the pattern found in the bilayer.

For 4-ML Mn/Fe(100) films the magnetic structure is even more complex. The favorite layered configuration is Fe$|uddu$ (see Table II, only results for the two most stable configurations are listed), but in-plane surface antiferromagnetism lowers the total energy by 11 meV/Mn. Magnetism in the subsurface layer is reduced to $-0.2\mu_B$, and the second subsurface layer is ferrimagnetic due to the strong FM coupling to the surface layer, with moments of $-0.76\mu_B$ and $1.44\mu_B$. The in-plane AFM surface layer and the ferrimagnetic second subsurface layer also show an appreciable buckling with amplitudes of about 0.08 Å. Interface coupling is FM, with bulklike Mn moments and slightly reduced Fe moments.

In a 5-ML Mn/Fe(100) film the layered configurations Fe$|uddud$ and Fe$|udduu$ differ in energy only by 2 meV/Mn. Both configurations are distinguished by strongly enhanced surface magnetism (to about $3.6\mu_B$), reduced magnetic moments in the subsurface layer and an oscillatory interlayer relaxation throughout the film. The results for films with 3 to 5 ML demonstrate that in addition to a strong FM Fe/Mn interface coupling, the second Mn layer always couples AFM to the Fe substrate. The results for the 4-ML and 5-ML films suggest also a strong AFM coupling of the third Mn layer to the substrate. The slight preference for the Fe$|uddud$ configuration results from the best match between the alternating AFM sequence issuing from the free surface and the interface coupling. Again in this case, in-plane AFM order in the surface layer lowers the total energy by 17 meV/Mn. The spin orientation in the deeper layers is the same as in the energetically most favorable layered phase, but the moments within layers differ in the third and fifth layers due to the long-range coupling to the large surface moments.

For a 6-ML Mn/Fe(100) films we have tested only the most promising layered configurations, and the total energy minimum was found for Fe$|uddudu$ order which is 21 meV/Mn lower in energy than the Fe$|uddudd$ configuration. Hence the sequence of the preferred layered configurations with increasing film thickness reveals that the addition of a single ML does not disturb the magnetic order of the underlying layers. The sequence is always Fe$|uddudu,\ldots$, even if truncated at a lower film thickness. The dd double layer following the ferromagnetically coupled interface layer seems to be a perturbation induced by competing medium

range Fe-Mn and Mn-Mn interactions, whereas farther away from the interface an alternating sequence of spin-up and spin-down layers builds up.

The results for the Mn/Fe(100) films may thus be summarized as follows.

(i) On average, the structure of the Mn films is almost ideally bcc, with only a minimal expansion along the tetragonal axis [the largest is found for a 3-ML film where $c/a = 1.013(c/a)_{\mathrm{bcc}}$ for a layered magnetic configuration and $c/a = 1.024(c/a)_{\mathrm{bcc}}$ if in-plane AFM is admitted]. The average atomic volumes of Mn in the films vary between 11.34 and 11.62 Å^3 depending on the film thickness and magnetic configuration, to be compared to the atomic volume of Fe with 11.33 Å^3. The Mn volume is slightly larger than the equilibrium volume of the tetragonal bulk phases. This is clearly due to a magneto-volume effect connected with surface-induced enhancement of magnetism.

(ii) Individual interlayer distances differ by up to ±12% from the ideal values. In general, distances between ferromagnetically coupled layers are expanded, distances between antiferromagnetically coupled layers contracted. This relaxation pattern cannot be related to the properties of the bulk phases, because at an axial ratio of about 0.71 the layered AFM phase is unstable and FM δ-Mn has a lower equilibrium volume than in-plane AFM δ-Mn (see Fig. 1). A correct assessment of interlayer relaxations is essential for determining the magnetic structure.

(iii) Although the geometric structure of the films is on average almost ideally bcc, the magnetic structure differs appreciably from that of bulk δ-Mn. The factors determining the magnetic order are: (iii-a) Only in the surface layer the AFM coupling between the enhanced surface moments is strong enough to impose a $c(2\times 2)$ in-plane AFM order. (iii-b) The strong FM Mn/Fe coupling at the interface with bulk-like Fe and Mn moments fixes the orientation of the Mn moments at the interface, irrespective of the film thickness. (iii-c) The strong FM interface coupling together with the alternating contraction and expansion of the interlayer distances stabilizes the layered AFM structure of the deeper layers of the film over the native in-plane AFM structure of bulk δ-Mn. Due to the variation of the interlayer distances, AFM interlayer coupling is preferred at the expense of AFM intralayer coupling. (iii-d) Both Fe-Mn and Mn-Mn exchange interactions are rather long-ranged and sometimes competing, even for layered configurations. Only part of this frustration signaled by quenched moments can be relieved by interlayer relaxations. (iii-e) There is always a substantial frustration connected with the transition from in-plane to layered AFM ordering, as illustrated by the strongly reduced magnetic moments in the subsurface layer and an eventual ferrimagnetism in the second subsurface layer. Nevertheless, these frustrations cost less energy than an enforced FM in-plane coupling between the large surface moments. (iii-f) It is noteworthy that for collinear configurations the addition of further Mn monolayers does not modify the magnetic structure of the underlying film, which is always Fe$|$*uddudu*,… . The outset of the sequence Fe$|$*udd* is likely induced by competing Fe-Mn and Mn-Mn interactions, in thicker films a layer-by-layer alternation is established. If in-plane antiferromagnetism in the surface is taken into account, a frustration in the subsurface layers is evident, but in thicker films the same Fe$|$*uddu*… configuration near the interface emerges.

C. Noncollinear magnetic structure, perpendicular coupling

The frustration evident at the transition from in-plane AFM at the free surface to layered antiferromagnetism in the deeper layers could eventually be relieved by adopting a noncollinear magnetic structure. We have investigated this possibility using the continuous vector field description of the magnetization density implemented in VASP (Ref. 91) and adding spin-orbit coupling. A fully relativistic calculation including spin-orbit coupling allows, in principle, to study also the magnetic anisotropy. However, for Mn where the orbital moment is exactly zero for the free atom according to Hund's rule, the magnetic anisotropy is expected to be very small. We have used the same slabs as in the collinear calculations, but because of the reduced symmetry we have now to sample over the full and not only the irreducible part of the Brillouin zone. During the iterations converging to a stable magnetic and geometric structure we have used 36 k points for obtaining a stable magnetic and geometric structure. The total energy of the final, relaxed configuration has been recalculated using 256 k points. For a 1-ML Mn/Fe(100) film the difference in total energy between these two calculations was rather small, 8 meV/Mn atom. We think that this degree of convergence on an absolute energy scale is sufficient to determine structural and magnetic energy differences to within 1 meV.

For a 1-ML Mn/Fe(100) film we have used three different initializations for the magnetic structure, two with the Fe moments initially aligned along the easy in-plane [100] direction and with either in-plane or perpendicular orientation of the Mn moments (which are aligned antiparallel to each other), the third with a random direction common to all the Fe moments. The geometric structure of the film was optimized simultaneously with the noncollinear magnetic structure. It turns out that the noncollinear solution has a lower energy by 75 meV/Mn atom compared to the most stable collinear in-plane AFM solution. Both calculations with in-plane Mn moments converge to the same magnetic structure with an angle of $2\varphi = 164.8°$ between nearest-neighbor Mn moments and a nearly perpendicular Mn/Fe coupling [the Fe-Mn angle is 82.4°, see Table III and Fig. 5(a) for details]. The total energies also agree within 0.3 meV/cell. The only difference is the orientation of the magnetic moments with respect to the easy axis. An initial orientation along the easy axis is maintained, but for a random initialization the torque forces acting on the magnetic moments are not sufficient to rotate the global magnetization into the easy axis. This is not surprising as the calculation of the very small in-plane magnetic anisotropy energy requires an exceedingly fine k-point mesh. In the unconstrained vector field description of the magnetization density this fine mesh is needed in the full, and and not only in the irreducible Brillouin zone.

If the Mn moments are initially oriented perpendicular to the magnetization of the substrate, the overall magnetic structure does not change dramatically: The moments in the

TABLE III. Noncollinear magnetic structure of a 1-ML Mn/Fe(100) film: in-plane components of orbital and spin moments m_l and m_s (in μ_B), the out-of-plane components are zero for m_l and below $0.003\mu_B$ for m_s; vertical interlayer relaxations $\Delta_{i,i+1}$ (in per cent of the interlayer distance in bcc Fe, d=1.415 Å). The last two columns show for comparison the results of the collinear calculation.

	i	m_{lx}	m_{ly}	$\lvert m_l\rvert$	m_{sx}	m_{sy}	$\lvert m_s\rvert$	$\Delta_{i,i+1}$	m_s	$\Delta_{i,i+1}$
Mn	1	−0.004	−0.019	0.019	0.458	−3.421	3.451	3.1	3.322	3.7
		−0.004	0.019	0.019	0.458	3.421	3.451		−3.585	1.3
Fe	2	0.050	0.005	0.050	1.615	−0.003	1.615	−1.7	1.422	−2.2
		0.050	−0.005	0.050	1.615	0.002	1.615		1.573	−2.2
Fe	3	0.049	−0.006	0.049	2.297	−0.255	2.311	1.6	2.302	2.9
		0.049	0.006	0.049	2.297	0.252	2.311		2.298	−0.5
Fe	4	0.052	0.003	0.052	2.299	−0.002	2.299	1.3	2.267	1.2
		0.052	−0.003	0.052	2.299	0.002	2.300		2.279	1.2

Fe substrate remain aligned in-plane in the easy direction. The positive and negative Mn moments are tilted by 7.6° with respect to the surface normal, the angle between the Mn moments is now 2φ=163.9°, the Fe-Mn angle is φ=81.9°. The magnitudes of the Mn and Fe moments at the interface are exactly the same as for in-plane orientation. The total-energy difference compared to in-plane Mn moments (i.e., the magnetic anisotropy energy MAE of the Mn film) is only ~0.1 meV/Mn atom. This is at the level (or even below) the numerical uncertainty. The exceedingly small MAE is a consequence of the very low orbital moments of Mn. In the Mn/Fe(100) films the orbital moments carried by the Mn atoms vary around $\sim 0.02\mu_B$, the Fe atoms of the substrate have orbital moments of about $0.05\mu_B$.

The comparison of the noncollinear and collinear calculations leads to the following conclusions: (i) The Mn/Fe coupling at the interface is almost perpendicular. Within a Heisenberg model and assuming only nearest neighbor exchange interactions, the magnetic energy may be written as

$$E = -2J_{\text{Mn-Mn}}m_{\text{Mn}}^2 \cos 2\varphi - 2J_{\text{Fe-Mn}}m_{\text{Mn}}m_{\text{Fe}} \cos \varphi. \quad (1)$$

The equilibrium condition with respect to the relative orientation of the moments

$$\frac{\partial E}{\partial \varphi} = 8J_{\text{Mn-Mn}}m_{\text{Mn}}^2 \cos \varphi \sin \varphi + 2J_{\text{Fe-Mn}}m_{\text{Mn}}m_{\text{Fe}} \sin \varphi = 0 \quad (2)$$

allows for the solutions φ=0 (collinear FM coupling), $\varphi = \pi$ (collinear AFM coupling), and

$$\cos \varphi = -\frac{J_{\text{Fe-Mn}}m_{\text{Mn}}m_{\text{Fe}}}{4J_{\text{Mn-Mn}}m_{\text{Mn}}^2}. \quad (3)$$

From a coupling angle of φ=82.4° and using the magnetic moments listed in Table III it follows that $J_{\text{Fe-Mn}} = -1.13\, J_{\text{Mn-Mn}}$, viz. the Fe-Mn coupling is ferromagnetic and stronger than the AFM Mn-Mn coupling. (ii) The differences in the absolute values of the Mn moments on the two inequivalent sites in the $c(2\times 2)$ cell which exist in the collinear calculation disappear if the magnetic moments are allowed to relax to a noncollinear orientation. This is accompanied by the disappearance of the buckling in the adlayer. In the Fe interface layer, the Fe moments relax to slightly larger values. (iii) The magnetic structure of the substrate remains almost exactly collinear except for the second Fe layer where the strong coupling to the Mn overlayer gives rise to a weak rotation of the Fe moments by about ±6° around the easy axis. (iv) Orbital moments in the Fe layers are about $0.05\mu_B$, but only $0.02\mu_B$ in the Mn layer. The orbital moments are misaligned with respect to the spin moments in the adlayer and close to the interface. On the Mn atoms the angle between spin and orbital moments is about 8°, so the angle between the orbital moments on the inequivalent Mn sites is 156° (i.e., substantially smaller than the angle between the spin moments).

Noncollinear solutions with in-plane and perpendicular Mn moments could also be determined for 2-ML Mn/Fe(100) films. The results are compiled in Table IV and Fig. 5(b). The noncollinearity affects both Mn layers, and also the top Fe layer. The angle between nearest-neighbor

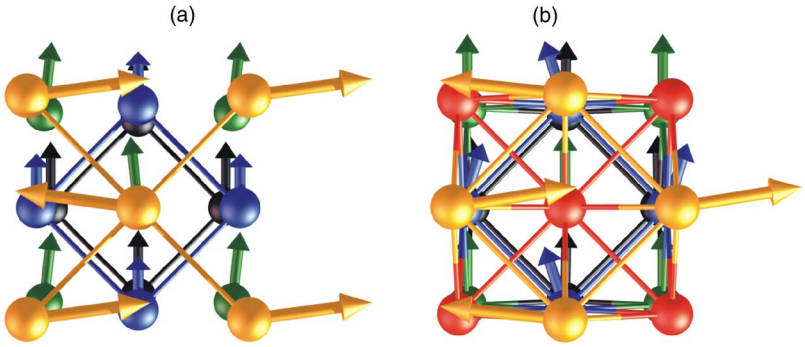

FIG. 5. (Color online) A top perspective view of the noncollinear magnetic structure of (a) a 1-ML Mn/Fe(100) film, (b) 2-ML Mn/Fe(100) film. Light grey (orange) balls display the top Mn atoms, subsurface Mn atoms in (b) are pictured in middle gray (red). Fe atoms are pictured in dark gray, the shading increases with the distance from the surface (in the color version first layer Fe atoms are colored in blue, second layer Fe atoms are green, and third layer Fe atoms black.

TABLE IV. Noncollinear magnetic structure of a 2-ML Mn/Fe(100) film: in-plane components of orbital and spin moments m_l and m_s (in μ_B), the out-of-plane components are zero for m_l and below $0.003\mu_B$ for m_s; vertical interlayer relaxations $\Delta_{i,i+1}$ (in per cent of the interlayer distance in bcc Fe, $d=1.415$ Å). The last two columns show for comparison the results of the collinear calculation.

	i	m_{lx}	m_{ly}	$\lvert m_l\rvert$	m_{sx}	m_{sy}	$\lvert m_s\rvert$	$\Delta_{i,i+1}$	m_s	$\Delta_{i,i+1}$
Mn	1	0.003	−0.017	0.017	0.458	−3.431	3.461	6.8	3.50	7.1
		0.003	0.017	0.017	0.458	3.432	3.462	6.9	−3.48	9.0
Mn	2	−0.004	−0.003	0.005	−0.126	−0.003	0.126	−6.6	0.08	−6.1
		−0.004	0.002	0.004	−0.127	−0.003	0.127	−6.6	−0.70	−6.3
Fe	3	0.042	−0.013	0.044	1.898	−0.612	1.994	2.3	2.05	2.0
		0.042	0.013	0.044	1.898	0.612	1.994	2.3	1.89	2.2
Fe	4	0.052	0.000	0.052	2.348	0.003	2.348	0.0	2.35	−0.3
		0.052	0.000	0.052	2.348	0.003	2.348	0.0	2.35	−0.5
Fe	5	0.049	0.000	0.049	2.336	0.040	2.336	3.2	2.32	2.7
		0.049	0.000	0.049	2.338	−0.040	2.338	3.2	2.35	3.1

moments in the top Mn layer is $2\varphi=164.9°$, i.e., exactly the same as for the Mn monolayer. Again there is no difference in the absolute values of the moments on the inequivalent Mn sites and no buckling, but due to the canting relative to an exactly antiparallel orientation, a small net surface-moment survives. The moments in the subsurface Mn layers are strongly quenched also in the noncollinear solution. Fe moments in the top layer of the substrate are misaligned by ±17.9° with respect to the FM easy axis. The angle between the Mn moments in the top layer and the Fe moments at the interface is 64.5°, i.e., the perpendicular coupling between Mn and Fe is disturbed by the presence of a second Mn layer. If the Mn moments are rotated into a perpendicular direction, the magnitudes of the moments remain unchanged, only the Mn-Mn, Fe-Fe, and Fe-Mn angles are slightly reduced to 134.6°, ±14.7°, and 52.6°, respectively. The electronic contribution to the MAE is 0.4 meV/Mn atom in favor of the perpendicular orientation, but this is far too small to override the dipolar energy favoring in-plane anisotropy.

For thicker Mn films convergence of noncollinear calculations turned out to be extremely slow. For a 4-ML Mn/Fe(100) a tolerably well-converged configuration shows the following qualitative features. (i) Mn/Fe coupling at the interface is predominantly ferromagnetic, but the Mn moments are canted relative to the Fe moments. (ii) As for the collinear calculation, the second Mn layer from the interface is ferrimagnetic, the Mn moments in this layer are roughly aligned with the moments in the Mn interface layer. In both layers the moments remain almost the same as in the collinear calculation. (iii) Magnetism in the subsurface Mn layer remains strongly quenched. (iv) The in-plane AFM at the surface is conserved. (v) The pattern of interlayer relaxations remains unchanged. The difficulty in achieving a converged noncollinear calculation arises from the decoupling of the surface layer from the deeper layers coupling to the substrate. In view of the stability of the layered AFM configuration in the deeper layers and the frustration at the transition to the in-plane AFM structure, a scenario of a perpendicular coupling between the in-plane ordered Mn surface layer and the layered structure deeper in the film is at least plausible.

D. Island formation and surface roughening

Under the assumption that islands formed on the surface of the film are sufficiently large such that contributions of the step edges and side facets of the islands to the total energy are negligible, the energy of a system consisting of more than one domain (e.g., regions of a clean Fe surface and regions of Mn islands of different thickness) is simply given by the weighted average of the surface energy of Fe and the energy of formation of Mn/Fe films of corresponding thickness. For the decomposition of a smooth Mn film of $(n+1)$-ML into n-ML thick underlayer and islands with a step height of h ML, we have to evaluate the energy difference for the surface atom

$$\Delta E_{\mathrm{isl}}^{h,n} = [(h-1)E_{n\mathrm{Mn/Fe}} + E_{(h+n)\mathrm{Mn/Fe}} - hE_{(n+1)\mathrm{Mn/Fe}}]/h. \tag{4}$$

The energies for the formation of two and three ML high islands deduced from our calculated total energies are summarized in Table V. For the evaluation of ΔE_{isl} we use the energies of the most stable magnetic configuration with an in-plane AFM ordered surface. The following picture emerges for 2-ML high islands. (i) A smooth 1-ML film is more stable than 2-ML islands on a clean Fe surface. The same result was also found by Asada *et al.*[72] (ii) A smooth 2-ML Mn film is less stable than 2-ML high islands on top of a compact Mn monolayer. (iii) Smooth 3-ML films are stable

TABLE V. Island formation energies ΔE_{isl} in meV/surface atom related to the decomposition of an $(n+1)$-ML thick film into a n-ML thick homogeneous film covered by h-ML high islands calculated according to Eq. (4) for one to three ML thick Mn films on Fe(100) substrate. Negative values indicate a tendency to island formation.

h	$n=0$	$n=1$	$n=2$	$n=3$
2	20	−34	82	−76
3	4	9	59	

TABLE VI. Magnetic moments m_i (in μ_B) in Fe_5Mn_3 multilayers and total energy difference (in eV/cell) relative to the ground-state configurations. The magnetic configurations are defined as follows: (i) Fe FM, Mn layered AFM, FM interface coupling, (ii) Fe FM, Mn in-plane AFM, (iii) FM, (iv) sublattice FM, AFM interface coupling, and (v) Fe FM, Mn layered AFM, AFM interface coupling (see text).

	layer	(i)	(ii)	(iii)	(iv)	(v)
Fe	1	2.06	2.06/2.06	2.13	1.99	2.00
Fe	2	2.24	2.31/2.33	2.30	2.40	2.38
Fe	3	2.28	2.33/2.32	2.32	2.33	2.37
Fe	4	2.24	2.31/2.33	2.30	2.40	2.38
Fe	5	2.06	2.06/2.06	2.13	1.99	2.01
Mn	6	2.12	1.78/−1.62	0.56	−1.75	−1.47
Mn	7	−1.00	1.04/−1.14	1.51	−0.65	1.35
Mn	8	2.12	1.78/−1.62	0.56	−1.75	−1.47
ΔE		0.000	0.230	0.232	0.516	0.918

against the formation of 2-ML high islands. (iv) 4-ML films are less stable than islands on 3-ML films. (v) 3-ML high islands are never stable.

Altogether, our results suggest Stranski-Krastanov growth, with 2-ML high islands appearing on an atomically smooth 1-ML Mn film. Smooth 3-ML films are in principle thermodynamically stable, but will probably never be formed because of the instability of 2-ML films. Our results give support to experimental reports[16,54] that island growth starts already at thicknesses around 3 ML.

V. Fe/Mn MULTILAYERS

Fe-Mn multilayers have been examined at the example of periodically repeated Fe_5Mn_3 multilayers. Investigation of in-plane AFM order and/or interface mixing requires models with a $c(2\times2)$ surface periodicity. To allow for an AFM interlayer exchange coupling between the Fe layers across the Mn spacer, some calculations with a cell doubled perpendicular to the layers have been performed. k-space integration is based on a $(10\times10\times3)$ grid (50 k points), for the doubled model we used a $(8\times8\times1)$ grid (16 k points).

A. Magnetic structure

In a first set of calculations we have examined the following five magnetic configurations with sharp Fe/Mn interfaces, in which the Fe layers are always ferromagnetic, but where the magnetic configuration in the Mn film changes: (i) layered AFM in the Mn layer, FM interface coupling, (ii) in-plane AFM in the Mn layer, (iii) FM ordering throughout the multilayer, (iv) both Fe and Mn layers are internally ferromagnetic, but Mn moments are oriented antiparallel to the Fe moments, and (v) layered AFM in the Mn layer, AFM Fe/Mn interface coupling. The interlayer spacing was fixed at the value $d=1.415$ Å calculated for bulk Fe, no relaxation was considered. The results are compiled in Table VI. The lowest energy is found for configuration (i), in which at the interface Mn moments are enhanced and Fe moments reduced compared to the bulk bcc phases. Configurations (ii) (with in-plane AFM in the Mn trilayer) and (iii) (completely FM) are both about 0.23 eV/cell higher in energy—this shows that to impose in-plane AFM (which is the magnetic ground-state of bulk δ-Mn) at the interface and to break the AFM coupling between the Mn layers costs about the same energy. Configuration (iv) with internally FM Fe and Mn layers and AFM interface coupling is 0.52 eV/cell higher in energy, but the highest energy difference of 0.92 eV/cell is found for configuration (v) preserving the layered AFM in the Mn trilayer but imposing an AFM coupling at the interface. The analysis of these magnetic energy differences confirms the dominant role of the FM Mn/Fe interface coupling, but also the long-range nature of the Mn/Fe coupling as evidenced by the strong increase of ΔE from configuration (iv) to (v).

For the configuration with the lowest energy, the configuration (i), we have investigated the effect of a complete relaxation of all interlayer distances (considering eventual change of the model size along the stacking direction of the layers), which are found to be quite modest. In the Fe_5 layer, the distances around the central Fe layer increase by 1.4%, the next Fe-Fe distances decrease by −1.2%. This is evidently due to a magneto-volume effect. As a consequence, the magnetic profile across the Fe layer becomes somewhat smoother, the Fe moment varies between $2.14\mu_B$ at the interface and $2.31\mu_B$ in the center. The Fe-Mn interlayer distance at the interface increases by 4%, the Mn-Mn interlayer distance decreases only very slightly by −0.2%. Mn moments increase to $2.20\mu_B$ at the interface and $-1.08\mu_B$ in the center of the trilayer. The energy gain by relaxation is modest (33 meV/cell), i.e., much smaller than the magnetic energy differences. Therefore the excited magnetic configurations of the multilayer have not been relaxed.

B. Interface mixing

Intermixing of Fe and Mn leads to a rather complex situation. The explored models with calculated magnetic moments are displayed in Fig. 6. For an all-FM configuration, intermixing with 50/50 Fe/Mn layers at both interfaces leads to a modest energy gain of 41 meV/cell. However, this energy is still higher than for an unmixed interface and layered AFM in the Mn trilayer. The magnetic moments in the mixed layers are $m_{Fe}=2.16\mu_B$ and $m_{Mn}=1.21\mu_B$ [see Fig. 6(b)]. Compared to the configuration with flat interfaces, the reduction of the magnetic moments is still more pronounced in the two layers occupied by Mn atoms only. Here the moments are $1.10\mu_B$ or $0.38\mu_B$. The situation is rather complicated if an AFM coupling between the Mn atoms is admitted. If the Fe_5 layers couple ferromagnetically through the Mn spacer [see Fig. 6(c)], the two pure Mn layers aligned antiparallel to the Fe and mixed layers are magnetically equivalent by symmetry. Their magnetic moments are considerably larger than in the all-FM configuration, but the energy is higher by 134 meV/cell, obviously owing to an unfavorable antiparallel coupling at the interface. It is instructive to com-

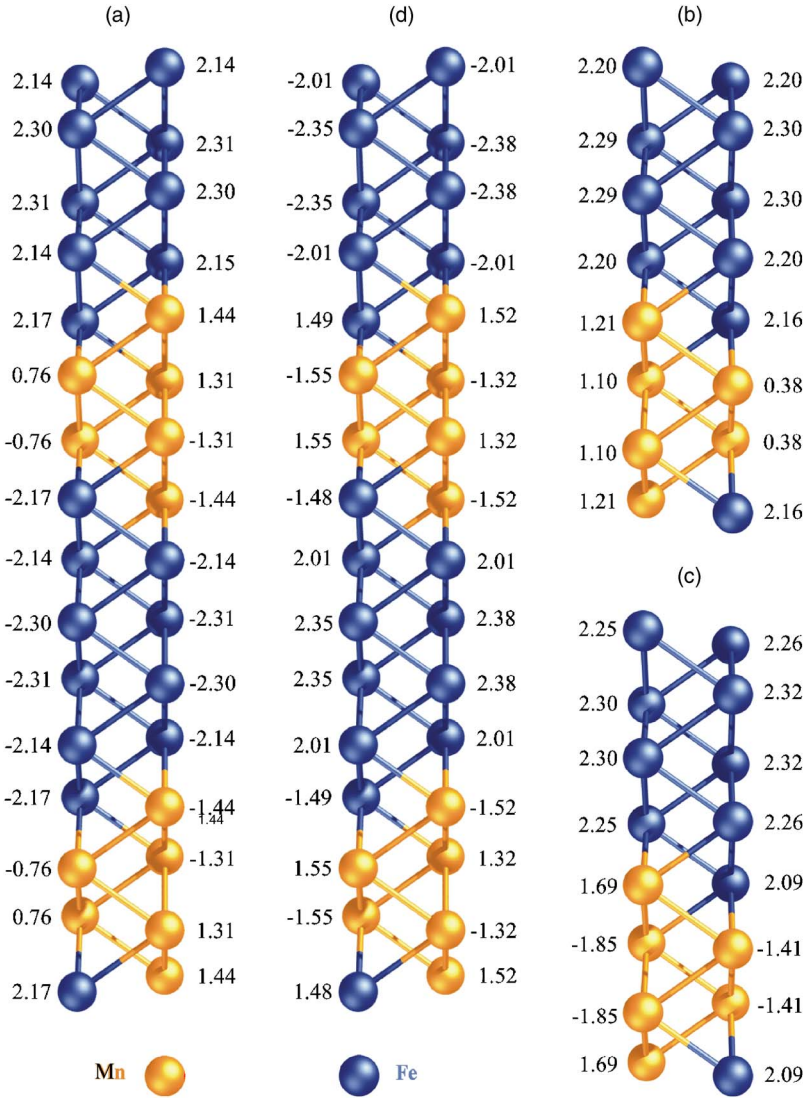

FIG. 6. (Color online) A side perspective view of the structure and magnetic moments (in μ_B) in Fe_5Mn_3 multilayers with 50/50 intermixed interfaces. Fe atoms are represented in dark grey (blue), Mn atoms in light grey (orange). (a) shows a configuration with FM interface-Mn coupling, AFM in Mn film, (b) an all FM configuration, (c) an AFM interface-Mn coupling, FM order in the Mn film, (d) an AFM interface-Mn coupling, AFM order in the Mn film. The configuration (a) has the lowest energy, that labeled by (d) the highest.

pare the configurations (a) and (d), both with an AFM Fe-Fe interlayer coupling through the Mn spacer, an antiparallel alignment of the moments in the two pure Mn layers, but with a distinct coupling between the intermixed and pure Mn layers. The configuration (d) with an AFM interface coupling of the moments in the mixed Fe-Mn layer with both the neighboring Fe and Mn layers has an energy higher by 1.7 eV/cell relative the configuration (a) where the Fe-Mn/Mn and Fe-Mn/Fe interface coupling is always FM. This conclusion points to a dominant role of the FM Fe/Mn interface coupling even if intermixing is admitted. To assess the effect of a chemical interface mixing alone, we compared two nonmagnetic models, the first one with sharp interfaces, and the second one with 50/50 intermixed interfaces with the result that the model with intermixed interfaces is less stable by 51 meV/cell. All in all, the most stable configuration among all investigated Fe_5Mn_3 multilayers, either with or without an interfacial mixing, is the configuration (i) in Table VI. Intermixing is not favored, though as the example of all-FM multilayers indicates, one can expect a slightly increased tendency to intermixing with the onset of magnetism.

VI. DISCUSSION AND CONCLUSIONS

We have presented a comprehensive investigation of the properties of tetragonal Mn in the bulk, at a free surface, in epitaxial ultrathin films on Fe(100), and Fe-Mn multilayers using a state-of-the-art all-electron full-potential density-functional approach allowing for a simultaneous optimization of all structural, electronic, and magnetic degrees of freedom. Our study has led to several novel aspects of the magnetism of the tetragonal phases of Mn. The first concerns the correlation between symmetry-breaking and magnetism. While the nonmagnetic and ferromagnetic cubic γ- and δ-Mn structures are at least locally stable, antiferromagnetic ordering induces tetragonal distortions. For γ-Mn two tetragonal phases compressed, respectively expanded along the tetragonal axis are energetically almost degenerate. The former adopts a layered AFM, the latter a $c(2\times2)$ in-plane AFM. Examination of helical magnetic configurations indicates that the layered AFM in tetragonally compressed γ-Mn is susceptible to long-period modulations. For tetragonally distorted δ-Mn, in-plane AFM is preferred over layered AFM, but helical magnetic configurations are even lower in energy (in

agreement with an earlier suggestion by Mohn *et al.*[32]). In-plane AFM in δ-Mn is also stable over an appreciable range of densities.[28]

Magnetism is strongly enhanced at the rather open (100) surface—from about $1.5\mu_B$ in the bulk to about twice this value. The magnetic enhancement is most pronounced for the nearly bcc phase showing in-plane AFM with a surface moment of $3.5\mu_B$. The magnetic moments show a slow oscillatory convergence towards the bulk value, accompanied by strong oscillatory relaxations of the interlayer distances. The surface-induced enhancement of magnetism is more modest (up to $\sim 2.7\mu_B$) on the surfaces of tetragonally distorted γ-Mn and accompanied by only weak interlayer relaxations. The most striking result, however, is that even for the tetragonally contracted γ-phase, in-plane AFM ordering in a buckled surface layer on top of a layered AFM bulk is stabilized by a reduced surface energy.

In-plane AFM in the surface layer also prevails in Mn/Fe(100) films, irrespective of their thickness, while the deeper layers adopt a layer-by-layer antiferromagnetic ordering. Different magnetic configurations of the Mn film show a very different pattern of interlayer relaxations. A full structural relaxation of the film and of the top layers of the substrate is required to achieve full convergence of the magnetic energy differences. On average, the geometric structure of the Mn films is rather close to ideal bcc—hence it is surprising that the films (except for the surface layer) adopt a layered AFM configuration which has been found to be unstable in bulk bcc Mn. Our calculations show a strong preference for a FM Mn/Fe coupling at the interface, and the layered magnetic structure imposed by the interface coupling propagates through the film. The conflict between the layered AFM structure in the deeper layers and the in-plane AFM in the surface layer leads to a strong quenching of the magnetic moments in the subsurface layer and to a certain buckling of the layers.

Our result of an in-plane AFM structure in the top layer of a Mn surface and of thicker Mn/Fe(100) challenges many accepted interpretations of the experimental results—theory has simply ignored this possibility thus far. However, there are also experimental indications of an in-plane AFM ordering on Mn surface—see, e.g. the investigations of Igel *et al.*[62] based on the capture of polarized electron by fast ions. Spin-polarized STM and STS experiments, combined with *ab initio* calculations of the simulation contrast, could provide a definitive answer. The most recent spin-polarized STM studies[17,64] show contrast reversal at steps in the Mn layers, but do not offer atomic resolution. The STM always images states at a certain distance from the surface. The examination of the surface-electronic structure of our films and a fundamental interpretation of the STM experiments must be left to further studies.

We have also searched for possible noncollinear magnetic configurations in the films, which could eventually relieve the frustration at the transition between in-plane and layered AFM. These calculations have been performed in a fully relativistic mode, including spin-orbit coupling. Because of the almost vanishing orbital moments of Mn and the consequently low anisotropy energies, convergence of the noncollinear calculations turned out to be very slow. For a 1-ML Mn/Fe(100) film we have found that AFM in the Mn layer is largely preserved, but the coupling between the Mn moments and the ferromagnetic moments of the substrate is now almost perpendicular, resulting from antiferromagnetic Mn-Mn and ferromagnetic Mn/Fe exchange interactions of comparable strength. An almost perpendicular coupling exists also between the top layer of a 2-ML Mn/Fe(100) film and the Fe substrate, but here the competing interactions induce also a slight canting of the Fe moments in the interface layer. While the noncollinear solution eliminates any difference in the magnitude of the magnetic moments within the same layer and any buckling, the magnetism in the subsurface layer is still almost completely quenched. Convergence of noncollinear calculations for thicker Mn films could not be achieved at a really satisfactory level, but it seems to be clear that the main result of the collinear calculations (in-plane AFM at the surface, layered AFM close to the interface) remains valid. The main difference is a certain canting of the Mn moments relative to the magnetization direction of the substrate producing a surface magnetic moment of $0.46\mu_B$ per Mn atom, which is aligned along the Fe magnetization.

We have also examined the thermodynamic conditions for interface mixing and growth. We find that at submonolayer coverage, very strong lateral interactions between the Mn atoms counteract the tendency towards exchange processes between isolated Mn adatoms and atoms of the substrate. Our results indicate that layer-by-layer growth is stable only in the monolayer limit, since already 2-ML films are less stable than islands on a smooth 1-ML film.

We have briefly explored the properties of Fe-Mn multilayers. The magnetic properties of the Mn spacer differ significantly from those of Mn films, because they are dominated by the strong exchange coupling at the interface. The magnetic frustration that is unavoidably present at an intermixed interface tends to stabilize smooth interfaces. Still, for the very thin Mn spacers considered here, the long-ranged exchange interactions always lead to competing exchange interactions and reduced magnetic moments in the Mn trilayer. The magnetism of the Fe layers on the other hand is found to be very robust, except immediately at the interface, Fe moments are always very close to their bulk values. As for the thin films, we have always found a strong preference for ferromagnetic Mn/Fe interface coupling, which is not perturbed if interface mixing occurs.

To summarize: The magnetic properties of the tetragonal phases of Mn, and in particular those of Mn/Fe thin films and …Fe/Mn/Fe/Mn… multilayers are found to be even more complex than suspected before. Our investigations have added some facets to an already sufficiently intricate problem: (1) For the tetragonal bulk phases, our calculations reveal a strong coupling between the broken tetragonal symmetry and the magnetic ordering, with a preference for $c(2\times 2)$ in-plane AFM in δ-Mn compressed and γ-Mn expanded along the tetragonal axis, and layered AFM in tetragonally compressed γ-Mn. For both phases we demonstrate a tendency towards long-period helical modulations of the magnetic structure. (2) The surface-induced enhancement of magnetism stabilizes in-plane AFM coupling in the top Mn layer of both a (100) Mn-surface and of thin

Mn/Fe(100) films. Although the geometric structure of the Mn films is nearly bcc on average (and hence the preference for in-plane AFM in bulk δ-Mn suggests the same magnetic structure in the film), the strong FM Mn/Fe interface coupling stabilizes a layered magnetic structure in the film. (3) This result is not much changed if magnetic noncollinearity is admitted, but as long as the in-plane ordered Mn-surface layer couples to the Fe substrate, the orientation between the surface- and substrate moments is essentially perpendicular. (4) Mn/Fe interface coupling is always ferromagnetic, in the thin films and in the multilayer, even if interface mixing occurs.

While it is not unexpected that there is a certain disagreement between different sets of experiments, and between experiment and theory for a system as complex as this, the disagreement between the theoretical results all based on density-functional theory might appear disconcerting. However, this agreement certainly does not signify a failure of a spin-density-functional theory, it is an expression of the complexity of the problem: (1) The strong correlation between the geometric and magnetic structures (as expressed by the coexistence of tetragonally compressed and expanded phases of γ-Mn with layered and in-plane AFM order, and the influence of interlayer relaxations on the magnetic phase stability of the thin films) suggests that simplified potential constructions such as the muffin-tin or atomic-sphere approximations are inadequate, a full-potential treatment is required. (2) The strong changes in the magnetic moments indicate that a very accurate description of the valence-core exchange interaction is mandatory. This requires an all-electron treatment (based, e.g., on a FLAPW or PAW approach), nonlinear core corrections to pseudopotential calculations are insufficient. Only a few of the studies presented so far fulfill both requirements. The challenge is now to reanalyze the most significant results (and in particular the topological information from STM and the spectroscopic information from STS) in the light of the theoretical results.

Note added in proof. The almost perpendicular orientation of the magnetic moments in a Mn/Fe(100) monolayer predicted in our study has very recently been confirmed experimentally using x-ray magnetic circular dichroism (XMCD) and linear dichroism (XMLD) spectroscopies.[93] These studies also suggest a local magnetic moment in the Mn monolayer larger than $3.5\mu_B$ - in excellent agreement with our calculated value of $3.45\mu_B$. The experimental investigations in this article have been supplemented by noncolinear spin-density-fuctional calculations using ultrasoft pseudopotentials, predicting an angle of 81° between the Mn and Fe moments — in perfect agreement with our result of 81.9°. The calculated magnetic moments in the Mn layer of $3.10\mu_B$ are distinctly lower than our values and the experimental estimates, but it is not clear whether a gradient-corrected or a purely local functional have been used.

Very surprising results have been found in *ab-initio* DFT calculations for tetragonal Mn films on W substrates.[94] Mn/W(110) films show $c(2\times2)$ in-plane AFM for up to 3 ML, and layered AFM in thicker films. Mn/W(100) films are predicted to be ferromagnetic up to 2 ML, the ferromagnetism being induced by the strong hybridization between the Mn- and W-d-bands across the interface. For the case of a single Mn monolayer on W(100), a similar conclusion was reached independently by Ferriani *et al.*[95] The unexpected ferromagnetism of Mn/W(100) films adds to the complexity of the magnetic phase diagram of tetragonal Mn.

ACKNOWLEDGMENTS

This work has been supported by the Austrian Science Funds under Project No. 16184-N02.

*Electronic mail: Juergen.Hafner@univie.ac.at
†Electronic mail: Daniel.Spisak@univie.ac.at

[1] *Ultrathin Magnetic Structures*, edited by J. A. C. Bland and B. Heinrich (Springer, Berlin 1994), Vols. I and II.
[2] See, e.g., J. Shen and J. Kirchner, Surf. Sci. **500**, 300 (2002); S. D. Bader, *ibid.* **500**, 172 (2002).
[3] L. P. Regnault, I. Zaliznyak, J. P. Renard, and C. Vettier, Phys. Rev. B **50**, 9174 (1994), and references cited therein.
[4] P. Grünberg, R. Schreiber, Y. Pang, M. B. Brodsky, and H. Sowers, Phys. Rev. Lett. **57**, 2442 (1986).
[5] S. S. P. Parkin, N. More, and K. P. Roche, Phys. Rev. Lett. **64**, 2304 (1990).
[6] M. N. Baibich, J. M. Broto, A. Fert, F. Nguyen Van Dau, F. Petroff, P. Etienne, G. Creuzet, A. Friederich, and J. Chazelas, Phys. Rev. Lett. **61**, 2472 (1988).
[7] G. Binasch, P. Grünberg, F. Saurenbach, and W. Zinn, Phys. Rev. B **39**, 4828 (1989).
[8] B. Dieny, V. S. Speriosu, S. S. P. Parkin, B. A. Gurney, D. R. Wilhoit, and D. Mauri, Phys. Rev. B **43**, 1297 (1991).
[9] J. Unguris, R. J. Celotta, and D. T. Pierce, Phys. Rev. Lett. **67**, 140 (1991).
[10] P. Grünberg, S. Demokritov, A. Fuss, R. Schreiber, J. A. Wolf, and S. T. Purcell, J. Magn. Magn. Mater. **104**, 1734 (1992).
[11] C. Turtur and G. Bayreuther, Phys. Rev. Lett. **72**, 1557 (1994).
[12] R. Pfandzelter, T. Igel, and H. Winter, Surf. Sci. **377–379**, 963 (1997).
[13] B. Heinrich, A. S. Arrott, C. Liu, and S. T. Purcell, J. Vac. Sci. Technol. A **5**, 1935 (1987).
[14] D. A. Tulchinski, J. Unguris, and R. J. Celotta, J. Magn. Magn. Mater. **212**, 91 (2000).
[15] E. Kentzinger, U. Rücker, W. Caliebe, G. Goerigk, F. Werges, S. Nerger, J. Voigt, W. Schmidt, B. Alefeld, C. Fermon, and Th. Brückel, Physica B **276–278**, 586 (2000).
[16] T. K. Yamada, M. M. J. Bischoff, T. Mizoguchi, and H. van Kempen, Surf. Sci. **516**, 179 (2002).
[17] T. K. Yamada, M. M. J. Bischoff, G. M. M. Heijnen, T. Mizoguchi, and H. van Kempen, Phys. Rev. Lett. **90**, 056803 (2003).
[18] D. Spišák and J. Hafner, Phys. Rev. B **55**, 8304 (1997).
[19] A. C. Lawson, A. C. Larson, M. C. Aronson, S. Johnson, Z. Fisk, P. C. Canfield, J. D. Thompson, and R. B. von Dreele, J. Appl. Phys. **76**, 7049 (1994).
[20] H. Yamagata and K. Asayama, J. Phys. Soc. Jpn. **33**, 400 (1972).

[21] M. O'Keefe and S. Anderson, Acta Crystallogr., Sect. A: Cryst. Phys., Diffr., Theor. Gen. Crystallogr. **33**, 914 (1977).
[22] H. Fujihisa and K. Takemura, Phys. Rev. B **52**, 13 257 (1995).
[23] H. Nakamura, K. Yoshimoto, M. Shiga, M. Nishi, and K. Kakurai, J. Phys.: Condens. Matter **9**, 4701 (1997).
[24] B. Canals and C. Lacroix, Phys. Rev. B **61**, 11 251 (2000).
[25] Y. Endoh and Y. Ishikawa, J. Phys. Soc. Jpn. **30**, 1614 (1971).
[26] F. R. de Boer, R. Boom, W. C. M. Mattens, A. R. Miedema, and A. K. Niessen, in *Cohesion in Metals*, edited by F. R. de Boer and D. G. Pettifor (North Holland, Amsterdam, 1988), Vol. I, p. 676.
[27] D. Hobbs, J. Hafner, and D. Spišák, Phys. Rev. B **68**, 014407 (2003).
[28] J. Hafner and D. Hobbs, Phys. Rev. B **68**, 014408 (2003).
[29] V. L. Moruzzi and P. M. Marcus, Phys. Rev. B **38**, 1613 (1988).
[30] S. L. Qiu, P. M. Marcus, and Hong Ma, J. Appl. Phys. **87**, 5932 (2000).
[31] V. L. Sliwko, P. Blaha, P. Mohn, and K. Schwarz, Int. J. Quantum Chem. **7**, 614 (1993).
[32] P. Mohn, K. Schwarz, M. Uhl, and J. Kübler, Solid State Commun. **102**, 729 (1997).
[33] T. Oguchi and A. J. Freeman, J. Magn. Magn. Mater. **46**, L1 (1984).
[34] S. L. Qiu, P. M. Marcus, and Hong Ma, Phys. Rev. B **62**, 3292 (2000).
[35] P. Krüger, O. Elmouhssine, C. Demangeat, and J. C. Parlebas, Phys. Rev. B **54**, 6393 (1996).
[36] M. Aldén, H. L. Skriver, S. Mirbt, and B. Johansson, Surf. Sci. **315**, 157 (1994).
[37] Y. Nishihata, M. Nakayama, N. Sano, and H. Terushi, J. Phys. Soc. Jpn. **63**, 319 (1988).
[38] W. F. Egelhoff, I. Jacob, J. M. Rudd, J. F. Cochran, and B. Heinrich, J. Vac. Sci. Technol. A **8**, 1582 (1990).
[39] D. Tian, S. C. Wu, F. Jona, and P. M. Marcus, Solid State Commun. **70**, 199 (1989).
[40] S. Andrieu, H. M. Fischer, M. Piecuch, A. Traverse, and J. Mimault, Phys. Rev. B **54**, 2822 (1996).
[41] T. G. Walker and H. Hopster, Phys. Rev. B **48**, R3563 (1993).
[42] R. Wu and A. J. Freeman, Phys. Rev. B **51**, 17 131 (1995).
[43] R. Wu and A. J. Freeman, J. Magn. Magn. Mater. **161**, 89 (1996).
[44] T. Asada and S. Blügel, Physica B **237**, 359 (1997).
[45] M. Eder, J. Hafner, and E. G. Moroni, Phys. Rev. B **61**, 11 492 (2000).
[46] D. Spišàk and J. Hafner, J. Phys.: Condens. Matter **11**, 6359 (1999).
[47] T. Flores, M. Hansen, and M. Wuttig, Surf. Sci. **279**, 251 (1992).
[48] M. Wuttig, C. C. Knight, T. Flores, and Y. Gauthier, Surf. Sci. **292**, 189 (1993).
[49] M. Wuttig, T. Flores, and C. C. Knight, Phys. Rev. B **48**, 12 082 (1993).
[50] M. Wuttig, B. Feldmann, and T. Flores, Surf. Sci. **331–333**, 659 (1995).
[51] Ch. Ross, B. Schirmer, M. Wuttig, Y. Gauthier, G. Bihlmayer, and S. Blügel, Phys. Rev. B **57**, 2607 (1998).
[52] S. K. Kim, Y. Tian, M. Montesano, F. Jona, and P. M. Marcus, Phys. Rev. B **54**, 5081 (1996).
[53] O. Rader, W. Gudat, D. Schmitz, C. Carbone, and W. Eberhardt, Phys. Rev. B **56**, 5053 (1997).
[54] M. M. J. Bischoff, T. Yamada, A. J. Quinn, and H. van Kempen, Surf. Sci. **501**, 155 (2002).
[55] R. Pfandzelter, T. Igel, and H. Winter, Surf. Sci. **389**, 317 (1997).
[56] E. C. Passamani, B. Croonenborghs, B. Degroote, and A. Vantomme, Phys. Rev. B **67**, 174424 (2003).
[57] T. Igel, R. Pfandzelter, and H. Winter, Surf. Sci. **405**, 182 (1998).
[58] P. Torelli, F. Sirotti, and P. Ballone, Phys. Rev. B **68**, 205413 (2003).
[59] J. Dresselhaus, D. Spanke, F. U. Hillebrecht, E. Kisker, G. van der Laan, J. B. Goedkoop, and N. B. Brookes, Phys. Rev. B **56**, 5461 (1997).
[60] S. Andrieu, M. Finazzi, F. Yubero, H. Fischer, P. Arcade, F. Chevrier, K. Hricovini, G. Krill, and M. Piecuch, J. Magn. Magn. Mater. **165**, 191 (1997).
[61] S. Andrieu, M. Finazzi, Ph. Bauer, H. Fischer, P. Lefevre, A. Traverse, K. Hricovini, G. Krill, and M. Piecuch, Phys. Rev. B **57**, 1985 (1998).
[62] T. Igel, R. Pfandzelter, and H. Winter, Phys. Rev. B **58**, 2430 (1998).
[63] Ch. Roth, Th. Kleemann, F. U. Hillebrecht, and E. Kisker, Phys. Rev. B **52**, R15691 (1995).
[64] U. Schlickum, N. Janke-Gilman, W. Wulfhekel, and J. Kirschner, Phys. Rev. Lett. **92**, 107203 (2004).
[65] S. Andrieu, E. Foy, H. Fischer, M. Alnot, F. Chevrier, G. Krill, and M. Piecuch, Phys. Rev. B **58**, 8210 (1998).
[66] B. Nonas, K. Wildberger, R. Zeller, and P. H. Dederichs, J. Magn. Magn. Mater. **165**, 137 (1998).
[67] B. Nonas, K. Wildberger, R. Zeller, and P. H. Dederichs, Phys. Rev. Lett. **80**, 4574 (1998).
[68] M. A. Khan, S. Bouarab, H. Nait-Laziz, C. Demangeat, and M. Benakki, J. Magn. Magn. Mater. **148**, 76 (1995).
[69] O. Elmouhssine, G. Moraitis, C. Demangeat, and J. C. Parlebas, Phys. Rev. B **55**, R7410 (1997).
[70] T. Asada, G. Bihlmayer, S. Handschuh, S. Heinze, Ph. Kurz, and S. Blügel, J. Phys.: Condens. Matter **11**, 9347 (1999).
[71] S. Mirbt, O. Eriksson, B. Johansson, and H. L. Skriver, Phys. Rev. B **52**, 15 070 (1995).
[72] T. Asada, S. Blügel, G. Bihlmayer, S. Handschuh, and R. Abt, J. Appl. Phys. **87**, 5935 (2000).
[73] S. Handschuh and S. Blügel, Solid State Commun. **105**, 633 (1998).
[74] S. Bouarab, H. Nait-Laziz, M. A. Khan, C. Demangeat, H. Dreyssé, and M. Benakki, Phys. Rev. B **52**, 10 127 (1995).
[75] A. Ernst, J. Henk, and R. K. Thapa, J. Phys.: Condens. Matter **17**, 3269 (2005).
[76] E. Martinez, A. Vega, R. Robles, and A. L. Vázqzez des Parga, Phys. Lett. A **337**, 469 (2005).
[77] M. Taguchi, O. Elmouhssine, C. Demangeat, and J. C. Parlebas, Phys. Rev. B **60**, 6273 (1999).
[78] S. T. Purcell, M. T. Johnson, N. W. E. McGee, R. Coehoorn, and W. Hoving, Phys. Rev. B **45**, 13 064 (1992).
[79] S. S. Yan, R. Schreiber, F. Voges, C. Osthöver, and P. Grünberg, Phys. Rev. B **59**, R11641 (1999).
[80] D. T. Pierce, A. D. Davies, J. A. Stroscio, D. A. Tulchinsky, J. Unguris, and R. J. Celotta, J. Magn. Magn. Mater. **222**, 13 (2000).
[81] J. C. Slonczewski, J. Magn. Magn. Mater. **150**, 13 (1995).
[82] G. Kresse and J. Furthmüller, Phys. Rev. B **54**, 11 169 (1996); Comput. Mater. Sci. **6**, 15 (1996).
[83] P. E. Blöchl, Phys. Rev. B **50**, 17 953 (1994).
[84] G. Kresse and D. Joubert, Phys. Rev. B **59**, 1758 (1999).
[85] J. P. Perdew and A. Zunger, Phys. Rev. B **23**, 5048 (1981).

[86] S. H. Vosko, L. Wilk, and M. Nusair, Can. J. Phys. **58**, 1200 (1980).
[87] J. P. Perdew, J. A. Chevary, S. H. Vosko, K. A. Jackson, M. R. Pederson, D. J. Singh, and C. Fiolhais, Phys. Rev. B **46**, 6671 (1992).
[88] J. X. Zheng-Johansson, O. Eriksson, B. Johansson, L. Fast, and R. Ahuja, Phys. Rev. B **57**, 10 989 (1998).
[89] C. Herring, in *Magnetism*, edited by G. T. Rado and H. Suhl (Academic Press, New York, 1966).
[90] M. Marsman and J. Hafner, Phys. Rev. B **66**, 224409 (2002).
[91] D. Hobbs, G. Kresse, and J. Hafner, Phys. Rev. B **62**, 11 556 (2000).
[92] M. Methfessel and A. T. Paxton, Phys. Rev. B **40**, 3616 (1989).
[93] C. Grazioli, D. Alfe, S. R. Krihsnkumar, S. S. Gupta, M Veronese, S. Turchini, N. Bonini, A. Dal Corso, D. D. Sarma, S. Baroni and C. Carbone, Phys. Rev. Lett. **95**, 117201 (2005).
[94] S. Dennler and J. Hafner (unpublished).
[95] P. Ferriani, S. Heinze, G. Bihlmayer and S. Blügel, Phys. Rev. B **72**, 024452 (2005).